Colloidal Phenomena in Relation to Non-Aqueous Bitumen Extraction

by

Leylisadat Mirmontazeri

A thesis submitted in partial fulfillment of the requirements for the degree of

Doctor of Philosophy

in

Chemical Engineering

Department of Chemical and Materials Engineering
University of Alberta

Abstract

The non-aqueous extraction process involves dilution of mined oil sand with an organic solvent (the "diluent"), followed by separation of unwanted materials (clays, silica sand, connate water, etc.) from the diluted bitumen. The main focus of this research is on the removal of fines solids from organic liquids, with particular emphasis on the interfacial science behind the process. Two possible scenarios were proposed for the removal of the solids: (a) through aggregation of the solids with one another (i.e. homo-aggregation), and (b) through attachment of the solids to water droplets (i.e. hetero-aggregation); both mechanism are to occur in non-aqueous environments.

The study of homo-aggregation was conducted on both macroscopic and microscopic length scales; the methods of investigation were, respectively, sedimentation test and the micropipette technique. It was discovered that the inter-particle forces were strongly dependent on the aromatic content of the diluent. This, we speculate, was due to the conformations of the bituminous molecules that were adsorbed on the solid surfaces. In particular, when in an aromatic environment, the adsorbed molecules are highly extended, thus forming steric barriers which prevent aggregation of the solids (via van der Waals attraction). It was also discovered that the rate of settling of the solids was strongly correlated with the adhesive force between the particles; the latter was measured using a micro-cantilever technique that was developed for this research. For example, in a purely aromatic diluent, the inter-particle force was zero; the

fine solids were stabilized and settled as individual particles. Thus, aromatic diluents are detrimental to homo-aggregation.

In the study of hetero-aggregation (i.e. attachment of solids to water droplets in non-aqueous liquids), the opposite was observed: it was the aliphatic diluent that created suppression of aggregation. The reason, which we discovered in this research, was due to a "rigid skin" that was created at the oil-water interface (i.e. the water droplet surface); this was likely due to the accumulation of colloidal asphaltene precipitates at the interface. We further demonstrated that addition of sodium naphthenates (SN), a class of surfactants indigenous to bitumen, could prevent formation of the rigid skin. However, SN had also the effect of significantly lowering the oil-water interfacial tension, which in turn weakened the solid-water attachment force.

We have also examined the role of aliphatic solvents in particle sedimentation. It was discovered that, although the precipitation of asphaltenes would suppress homo-aggregation of the unwanted solids, the "network" of precipitates was capable of trapping the particles, which led to their separation — albeit at a slower rate compared to that by homo-aggregation. (This study provided the first mechanistic insight into the so-called "paraffinic froth treatment" process that is widely employed in the oil sands industry.)

Preface

The research conducted for this thesis was an original work by Leylisadat Mirmontazeri; Appendix B of this thesis is a collaboration between the author and Dr. Shima Afshar. This section is published in *Fuel* 128 (2014) 1-6; it is coauthored by L. Mirmontazeri, S. Afshar and A. Yeung. The first and second authors had equal contributions in this paper; Dr. Yeung was the supervisor.

Acknowledgments

I would like to express my sincere gratitude to Dr. Anthony Yeung and Dr. Qi Liu for their bright supervision, persistent encouragement and inspiring guidance throughout the course of this work. I appreciate their creative insights and ideas which provided a great learning experience during this research.

Special thanks to Dr. Yeung for not only being my mentor but also a close friend during all of these years. I truly value everything I have learned from him. It will forever remain a major contributor behind my success and achievements.

I also would like to thank my colleagues Shima Afshar, Mehdi Omidghane, Maryam fotovati, Feng Lin, Farnaz Mani, Amin Karkooti, Ying Jin and Weikang Liu for their help and assistance during this time.

My deepest gratitude goes to my mom, dad and my brother for their limitless love. I would like to thank them for being a great encouragement in my life. Special thanks to Ardalan, for his endless love, energy and support in the highs and lows of my graduate experience.

Table of Contents

List of tables

List of Figures

Nomenclature

A	Hamaker constant	(J)
a	Radius	(m)
D	Separation distance	(m)
d	Hydrodynamic diameter of the particle	(m)
E	Interaction energy	(J)
F	Force	(N)
g	Acceleration due to gravity	(m/s^2)
K_b	Cantilever stiffness	(N/m)
P	Pressure	(Pa)
Q	Electric charge	(C)
R	Radius of curvature	(m)
Re	Reynolds number	
U_T	Particle settling velocity	(m/s)
γ	Interfacial tension	(N/m)
δ	Cantilever deflection	(m)
ε	Dielectric constant, volume fraction occupied by the fluid	
ε_0	Permittivity in vacuum	($C^2/N.m^2$)
μ	Viscosity	(Pa.s)
ρ	Density	(kg/m^3)

1. Introduction

1.1 Water-Based Bitumen Extraction

The Canadian oil sands, with 179 billion barrels of recoverable oil, is one of the largest petroleum resources in the world [1]. On the global scale, this amount has put Canada in the second place after Saudi Arabia (with a reserve of 260 billion barrels). At present, production of more than one million barrels of high-grade synthetic crude oil per day has already made this country the largest foreign oil supplier for the United States. According to the National Energy Board of Canada, this current rate of oil production is expected to triple by year 2015 [2].

Current methods of extracting bitumen[†] from the Athabasca oil sands are characterised as 'water-based': Mined oil sand ores are first slurried in heated water; mechanical energy in the form of agitation and/or pipeline transport is introduced into the slurry to separate bitumen from the sand grains. The mixtures are then pumped into large water-filled vessels to achieve bitumen separation from the sand grains through a flotation process. In addition to problems with oil losses through the reject solids (which can result in economic and environmental issues), consumption of excessive amounts of water and energy by the water-based extraction method is also a major drawback. Therefore, although the economic benefits of the oil sands industry are undeniable, its environmental

[†] Bitumen is an extra heavy form of crude oil that is abundant in the Athabasca oil sands.

impact is also considerable. Of particular concern is the consumption of large volumes of water by the water-based extraction method. This water consumption can result in the following environmental problems [1]:

- The Athabasca River — the main source of water for current oil sands operations — also supplies fresh water to the city of Fort McMurray, its neighbouring communities and the Lake Athabasca extended deltas. Current rate of water consumption has negative impact on these communities and ecosystems. For instance, there is already reported damage to the habitat of many fish species. (Approved oil sands projects are licensed to draw 349 million m^3 of fresh water per year from the Athabasca River. This amount of water is roughly the water usage by a city twice the size of Edmonton [1].)

- The enormous amount of energy required to heat the process water results in issues such as greenhouse gas emissions and depletion of natural gas resources.

- About 90% of the contaminated process water cannot be released back to the environment and is instead kept in large tailings ponds. This raises several environmental issues, such as contamination of surface water and surrounding soils.

1.2 Solvent-Based Bitumen Extraction

With projected increase in oil sands production, the above-mentioned problems will become even more critical. Therefore, an alternative *solvent-based* extraction method is vital as a substitute for the current water-based method. The basic principles of such a non-aqueous technology are simple. Initially mined oil sand is mixed with an organic solvent that dissolves the bitumen component. Then, the large insoluble clay and sand particles are removed by passing through an initial stage of separation; this can be achieved by traditional separation methods such as centrifugation, filtration, or other means (see Figure 1.1). The solids-free diluted bitumen is then put through a distillation process, where the solvent is recovered and the product (extracted bitumen) is sent downstream for further upgrading.

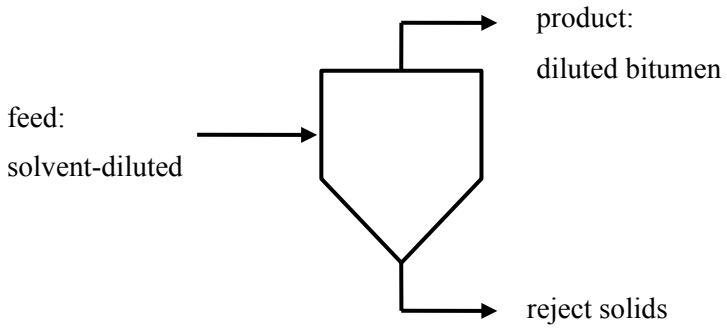

Figure 1.1. Schematic view of a non-aqueous (solvent-based) process: coarse solids are separated from solvent-diluted bitumen by sedimentation or other conventional means.

Various non-aqueous processes had been proposed for bitumen extraction in the past decades. One example is the solvent extraction-spherical agglomeration (SESA) process which exploits the oil-water interface for capturing solids [3-7]. In this method, addition of small amounts of water, along with mechanical agitation, helps to coagulate the solid particles. In particular, the water droplets act as binders that trap hydrophilic solids and create easily removable solid-water agglomerations. Unfortunately, this method, along with other proposed techniques, had not progressed beyond pilot tests. The two main obstacles to all the proposed non-aqueous processes are:

1. Failure to remove fine solids from the oil phase (i.e. diluted bitumen) will result in fouling and general contamination of upgrading facilities.
2. Failure to recover the residual oil trapped between reject sand grains will result in solvent loss and large scale environmental pollution.

To develop a successful solvent-based extraction process, the mechanisms which underlie the above two obstacles should be understood before any commercial implementation is attempted.

This PhD research is mainly focused on the first obstacle mentioned above, namely, the removal of unwanted particulates from a diluted bitumen medium. In addition, a brief experimental campaign was also dedicated to the study of the recovery of residual oil trapped between reject solids (second obstacle mentioned above).

Removal of fine particulates from diluted-bitumen (i.e. the product stream) is quite challenging. The majority of these particulates are fine clays and silica particles with sizes ranging from 10 nm to 10 μm. It should be mentioned that conventional separation methods (e.g. centrifugation or filtration) are only able to remove particles larger than about 100 microns. The usual methods of separation are not suitable for removal of the remaining fine particulates. However, if we could create conditions under which the suspended particulates destabilize (in a colloidal sense) and aggregate, it would then be possible to eliminate the aggregates using conventional methods of separation.

Two promising mechanisms of removing fine solids in non-aqueous environment are: (a) homo-aggregation of the solids, which is the adhesion between solid particles, and (b) hetero-aggregation of solids — in this case, the use of emulsified water as 'collectors' of the solid particles. It is clear that the colloidal forces between particles will play a central role in their aggregation. The most direct way of examining colloidal interactions in oil media is through measurement of inter-particle forces. Therefore, our intension in this study is to focus on fundamental interfacial science and understand the basic interactions between (a) solids in non-aqueous media, and (b) solids and oil-water interface.

1.3 Application to Paraffinic Froth Treatment

As mentioned in Section 1.1, in the water-based method of extracting bitumen, a mixture of oil sand and water is introduced into the water-filled vessels to create

bitumen separation by flotation (i.e. aerated bitumen reported to the top of the vessel as a froth, while the heavy sand grains exit from the bottom as tailings). The oil-rich froth, however, still contains some unwanted material such as water and solids. To address this problem, the bitumen froth is diluted with an organic solvent in the so-called "froth treatment" process. Due to the lowered density and viscosity of the hydrocarbon (diluted bitumen), it is possible to use conventional separations techniques, such as gravity settling and centrifugation, to remove emulsified water and coarse solids from the mixture [8]. Removal of fine particulates in the froth treatment process strongly depends on the type of the diluent solvent. In naphthenic froth treatment, the bitumen is diluted with naphtha followed by multistage gravity settling and/or centrifugation; the resulting diluted bitumen product, unfortunately, still contains micron-sized water droplets and fine solids which could lead to problems in downstream upgrading facilities (such as catalyst fouling) [9-11]. In contrast, dilution of the bitumen with a paraffinic solvent (paraffinic froth treatment of "PFT") results in the precipitation of a fraction of bitumen called *asphaltene*; interestingly, all the unwanted particulates are also somehow collected and removed with the asphaltene precipitates. This leads to a more efficient cleaning process which requires only simple gravity settling. Despite many studies on the PFT process, its underlying mechanism is still poorly understood [9, 12, 13]. It is believed that during the PFT process, asphaltene precipitates adhere to one another and form a network; all unwanted particulates are irreversibly trapped by the settling asphaltene network which

results in cleaner bitumen froth products [14]. A sketch of this phenomenon is shown in Figure 1.2(a). However, in an earlier study by our group, Jin et al. (2011) have demonstrated that in paraffinic solvents (such as *n*-heptane), bitumen-coated solids could homo-aggregate (i.e. adhering to one another) through what was believed to be van der Waals attraction [15]. This observation suggests homo-aggregation of solids as an effective parallel mechanism in PFT; a sketch of this alternate mechanism is shown in Figure 1.2(b). The question is: how will the precipitation of asphaltene affect the homo-aggregation of solids? In other words, is the removal of particulates during PFT entirely due to entrapment of fine solids by the precipitated asphaltene networks, or are solids homo-aggregation and asphaltene network entrapment both occurring simultaneously? These questions will be answered in the course of this study.

Figure 1.2. Possible mechanisms for paraffinic froth treatment: (a) Asphaltene network entrapment of particulates,(b) homo-aggregation of the fine solids.

This thesis is organized as follows: Chapter 2 will provide background information on the settling behavior of particles and the techniques of determining settling rates. In this chapter, inter-particle interactions and different available techniques of measuring colloidal forces are also introduced. Chapter 3 covers the experimental approaches that are used to study the physics of particle-particle

interactions, as well as particle attachment at the oil-water interface. These approaches include adhesive force measurements using the novel micro-cantilever technique, followed by bench-scale settling tests using the sedimentation balance. The experimental results and discussion of the underlying mechanisms are provided in Chapter 4. Finally, the contributions of this research and suggestions for future work are discussed in Chapter 5.

It is noted that the work presented in the main body of this thesis was motivated by the need to remove fine solids from the product stream (diluted bitumen) of a non-aqueous extraction process (see Figure 1.1). In addition to this, a brief case study was made on the recovery of residual hydrocarbon from the reject sand grains (also shown in Figure 1.1) using water and surfactants; for completeness, this case study is presented in Appendix B.

2. Literature Review

2.1 Settling Behaviours in Diluted Bitumen

As mentioned in Chapter 1, removal of suspended fine solids from the oil phase (diluted bitumen) is one of the main challenges in non-aqueous bitumen extraction. The coarse solids are easily removed by separation methods such as filtration or centrifugation. However, fine solid particles, which are mainly clays, are not susceptible to conventional separation methods. These remaining solids can lead to problems in the downstream upgrading facilities, such as fouling of the catalysts. Therefore, it is imperative to study the mechanisms behind aggregation and sedimentation of fine particles in non-aqueous (i.e. organic) liquids to improve removal of fine solids. In this section, the basic concepts of sedimentation and aggregation of solids will be discussed.

2.1.1 Sedimentation

Consider an individual particle undergoing settling in a fluid in a gravitational field. The particle reaches its terminal velocity when the frictional force on the particle is balanced by the gravitational force. The particle terminal velocity for systems with small Reynolds number can be calculated based on the Stokes' law:

$$U_T = \frac{d^2 g}{18\mu}(\rho_p - \rho_f) \qquad \text{Equation 2.1}$$

where U_T (m/s) is the particle terminal settling velocity, d (m) is the hydrodynamic diameter of the particle, g (m/s^2) is the gravitational acceleration, ρ_p (kg/m^3) is the density of the particles, ρ_f (kg/m^3) is the density of the fluid, and μ (Pa·s) is the fluid viscosity.

In a real process, however, the particles are often in a suspension and are spaced not far from one another. The close vicinity of neighbouring particles creates significant interaction of the solids with each other and will affect their motion and hinder their settling [16, 17]. The sedimentation rate of particles under this "hindered settling" condition can be significantly less than that for particles that are not affected by the presence of neighbouring particles (i.e. the free settling condition). For systems undergoing hindered settling, Richardson and Zaki (1954) suggested the following empirical relation:

$U = U_T \varepsilon^n$ (n= 4.65 for Re < 0.3 and n= 2.4 for Re > 500) Equation 2.2

where U (m/s) is the particle settling velocity, ε is the volume fraction occupied by the fluid, and Re is the Reynolds number based on the particle diameter and the free settling Stokes velocity [18].

2.1.2 Aggregation

Aggregation of fine particles occurs when the particles collide and adhere to one another and form flocs. These flocs commonly have loose and porous structures. The effective density of these aggregates is intermediate between the density of the particles and the trapped liquid inside. These aggregates then begin to settle

as a result of the density difference between the aggregate and the surrounding liquid. Aggregation and sedimentation of particles in colloidal suspensions is of interest to industrial applications such as conventional solid-liquid separation (e.g. sedimentation, filtration and waste water treatment). The effectiveness of gravity settling, perhaps the simplest form of separation processes, is a strong function of the propensity for aggregate formation. Particularly, the settling rate of aggregates depends on the initial solids concentration and inter-particle attraction. Therefore, one can optimize the settling rate by controlling initial solids concentration and chemical environment that will enhance solid aggregation.

The prerequisite for aggregation of two particles is their collision in the suspending fluid. The most important mechanisms of particle collision are:

1- Perikinetic aggregation, which is due to the random Brownian motions of the particles.
2- Orthokinetic aggregation, driven by shear flow of the suspending fluid.
3- Differential settling, which occurs when bigger flocs, which settle at higher downward velocities, catch up to smaller flocs and result in collisions.

Once the particles are brought into close contact by the above mechanism(s), short range inter-particle forces begin to play a critical role. Depending on the suspending liquid, forces of various origins (e.g. van der Waals attraction and electrostatic repulsion) can become relevant. More discussions on the different types of inter-particle forces are given in Section 2.2.

2.1.3 Methods of Quantifying Settling Rates

2.1.3.1 Optical Method

Visualization is the most common method of measuring settling rate of particles. This method is based on tracking of the "mud line" (i.e. the boundary which separates clear liquid at the top and "muddy" suspension at the bottom) using optical instruments. A schematic of the experimental setup is seen in Figure 2.1.

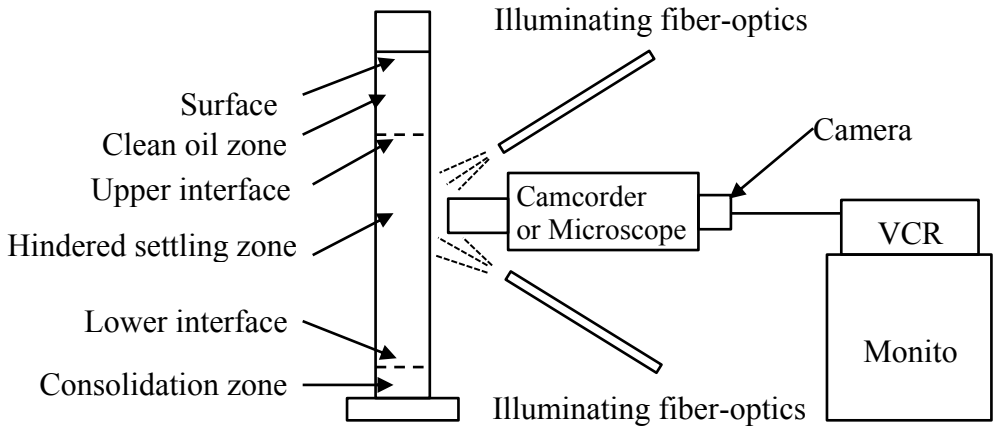

Figure 2.1. Experimental setup for settling tests measurements through optical method [9].

The well mixed solution is introduced quickly into a settler. The movement of the mud line, which is illuminated using two fiber-optic bundles, is recorded with a camcorder or light microscope. By analyzing the recorded images, the position of the mud line is plotted versus time. The settling rate is commonly taken to be the descending velocity of the mud line interface [9, 19].

This method seems to be a convenient and straightforward way of quantifying the settling rate for systems with clear and transparent suspending liquids. However, in opaque and dark solutions (e.g. sedimentation of solids in crude oil), it is rather difficult to follow the mud line movement.

Another important consideration is that accurate determination of the mud line location requires that the interface be sharp and well-defined. However, for systems with a broad particle size distribution, this interface often becomes more dispersed (i.e. blurred) as solids settle at different velocities (bigger particles settle faster and leave the smaller ones behind, thus creating a "smeared" mud line, especially at later stages of the sedimentation process).

In the present research, the suspending liquid (diluted bitumen) is very dark and opaque, and the mud line becomes dispersed very early on. Therefore, the optical method is not effective. For quantification of settling rates, we will, instead, make use of a simple device called the sedimentation balance.

2.1.3.2 Sedimentation Balance

In dark suspending liquids such as diluted bitumen, observing the settling solids is almost impossible; a simple and effective alternative is to use the sedimentation balance. In this method, the settling rate is quantified by collecting the solids at a fixed depth in the settling vessel using a small plate that is connected to a micro-balance (KRÜSS K100). The suspension is initially stirred so that the particles are distributed evenly. When the stirring stops (at time $t = 0$), settling will begin.

As the solids collect on the plate, the weight on the balance continuously increases until it reaches a constant value (i.e. no more particles above the collector). A plot of the mass *m* of the solids sediment (at a fixed depth) versus time *t* can provide useful information on the sedimentation process. The time at which the plot reaches a plateau will be called the "settling time," and the inverse of the settling time can be used as a measure of the settling rate. A more detailed description of this method will be given in Chapter 3. For a schematic diagram of this method, see Figure 3.1.

2.2 Colloidal Interactions

The stability of suspended particles against aggregation is determined by inter-particle colloidal forces. These forces are short ranged (< 0.1 μm) and therefore, in most cases, effective on length scales that are much smaller than the size of the particles. In comparison to covalent or hydrogen bonds, they are considered relatively weak forces. The most common types of colloidal forces are the attractive van der Waals (VDW) forces and the repulsive electric double layer (EDL) forces; both of these interactions are Coulombic in origin.

2.2.1 Coulombic Interaction

Coulombic forces stem from electrostatic interaction between two charged particles. As two like charges are brought together, they will repel each other; unlike charges, on the other hand, lead to attraction. The Coulombic force F between two point charge particles separated by a distance D is :

$$F = \frac{Q_1 Q_2}{4\pi\varepsilon\varepsilon_0 D^2}$$ Equation 2.3

where Q_1 and Q_2 are the magnitudes of the two charges (in coulombs), ε_0 is permittivity in vacuum (8.854×10^{-12} $C^2/N.m^2$), and ε the dielectric constant of the surrounding medium [20].

2.2.2 Van der Waals Attraction

This is a universal attractive force which acts between any two *point* particles (e.g. atoms or molecules). This force arises as a result of permanent or instantaneous dipoles. Two neighbouring molecules sample (i.e. go through) all possible relative orientations owing to Brownian motions and/or electrons orbiting around the nucleus, giving rise to instantaneous Coulombic forces that are either attractive or repulsive. *On average,* the van der Waals (VDW) interaction is *always attractive*, and the interaction energy E varies as $E \sim 1/D^6$, where D is the separation distance between the two point entities. The attraction between macroscopic particles depends on the particles size, the distance between them, and the composition of the particles [20].

Based on Derjaguin's approximation, the VDW interaction between two spherical particles of radii R_1 and R_2, in the case when the gap width D is much less than R_1 or R_2, is given by:

$$E_{VDW} = -\frac{A}{6D} \cdot \frac{R_1 R_2}{R_1 + R_2}$$ Equation 2.4

where A is the Hamaker constant (which relates to the properties of the interacting bodies and the intervening medium). The VDW force is the negative derivative of the energy:

$$F_{VDW} = -\frac{A}{6D^2} \cdot \frac{R_1 R_2}{R_1 + R_2}$$ Equation 2.5

Likewise, the VDW energy and force between a sphere and a planar surface is [20]:

$$E_{VDW} = -\frac{A\,R}{6\,D} \quad \text{and} \quad F_{VDW} = -\frac{A\,R}{6\,D^2}$$ Equation 2.6 and 2.7

2.2.3 Electrostatic Double Layer Repulsion

When two charged surfaces are immersed in an electrolyte (i.e. water with dissolved ions), a non-uniform distribution of ions forms near the particle surfaces. Owing to Coulombic attraction, the charge on the particle surface will be balanced by oppositely charged counterions from the solution, resulting in a high concentration of counterions near the particle surface. The concentration of counterions drops off exponentially with increasing distance from the surface. The characteristic length of this exponential decay is called the *Debye length* ($1/\kappa$); where κ varies as (ion concentration)$^{1/2}$. When two charged surfaces are brought close enough to each other such that the separation distance is of order $1/\kappa$, the concentration of counterions in the gap will be higher than that in the

bulk. This will give rise to an *osmotic pressure* in the gap, which acts to push the two surfaces apart. This is the origin of the electric double layer (EDL) repulsion [20].

2.2.4 Combined Interactions: The DLVO Theory

The colloidal stability of a given dispersion is a consequence of the interplay between van der Waals (attractive) and electric double layer (repulsive) energies. The repulsive force acts as a dispersion stabilizer, while the attractive force destabilizes the dispersed phase. This theory is named DLVO, in honour of the four scientists — Derjaguin and Landau from the USSR, and Verwey and Overbeek from the Netherlands — who independently developed such a theory.

2.2.5 Macromolecules Adsorbed on Solid Surfaces

Another common type of colloidal interaction in non-aqueous systems involves adsorbed large molecules or "macromolecules"; such interactions are steric in nature [11]. Bitumen consists of fairly large and heavy molecules that are formed from aliphatic side chains, polar heteroatoms and some metals. Adsorption of some portions of these macromolecules onto the surfaces of suspended solids can significantly affect particle-particle interactions. The "quality" of the solvent (using terminology from polymer physics), and the amount of adsorbed macromolecules, are two factors that determine such interactions.

2.2.6 Steric Repulsion

Drawing analogies from polymeric systems, macromolecules can adsorb onto solid surfaces and form tails and loops. The tails and loops will contribute to a "brush" as the adsorbed molecules are closely packed. Pressing together two covered surfaces (i.e. as two particles closely approach one another) will cause the brushes to repel each other, thus leading to a short-range steric repulsion between the particles [10].

2.2.7 Cross Bridging

When macromolecules are sparsely adsorbed onto suspended particles, an opposite effect can result: The same macromolecule may latch onto two adjacent particles, resulting in a cross-bridging phenomenon (Figure 2.2). This is effectively an attractive interaction; it occurs at particle separations that are comparable to the size of the macromolecule [10]. (Note that the "size" of the macromolecule is a function of its conformation, which in turn depends on the "quality" of the surrounding solvent.)

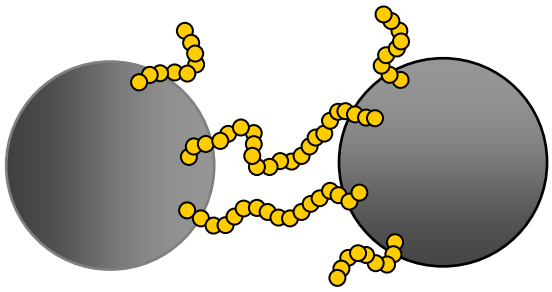

Figure 2.2. Polymer cross-bridging between two particles.

2.3 Colloidal Forces in a Non-Aqueous Medium

As was mentioned earlier, the electric double layer repulsion is of great importance in systems that involve aqueous or polar media. However, as ions have very low solubility in non-polar liquids (which is the main focus of our study), the diffuse double layer will not form. Indeed, charged particles suspended in a non-aqueous environment will often be subjected to Coulombic interactions, which are always "screened" by counterions in aqueous media.

2.4 Measurement of Surface Forces

The forces between colloidal particles dominate the behaviour of the system. Here, some of the most common methods of surface force measurements are described. In addition, a novel technique employing micropipettes to measure inter-particle forces is introduced.

2.4.1 Surface Force Apparatus

This method is capable of directly measuring the surface forces in liquid and vapour with high precision. The surface force apparatus (SFA) consists of two crossed mica cylinders (Figure 2.3). One of the cylinders is connected to a piezoelectric translator which controls the separation distance between the cylinders; the other cylinder is mounted to a spring. The separation of the two cylinders can be measured with an optical technique (with angstrom precision). Based on the deflection of the spring, the force can be obtained [20, 21].

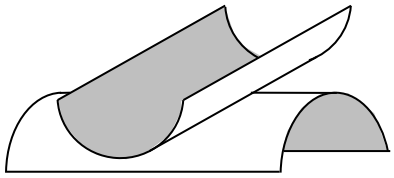

Figure 2.3. Schematic of the crossed cylinders in a surface force apparatus.

2.4.2 Atomic Force Microscope

The atomic force microscope (AFM) is another direct surface force measurement technique; it determines the colloidal force between a planar surface and an individual colloid particle. The procedure begins with attaching a spherical particle or probe to the tip of a force-sensing cantilever. This cantilever is positioned over a sample surface, and the entire assembly can be immersed in a liquid (Figure 2.4). When the tip approaches the sample, surface forces will cause deflection of the cantilever. Employing Hooke's law, the surface forces can be determined as a function of separation distance [20, 22].

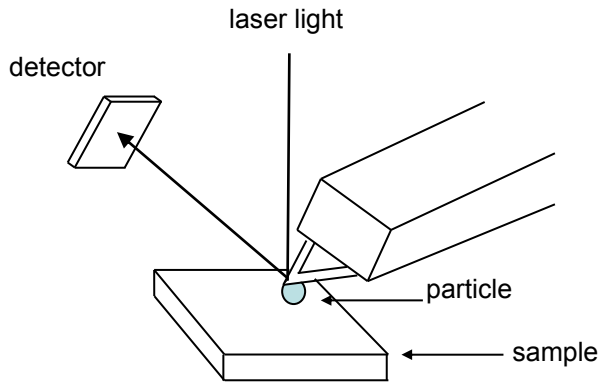

Figure 2.4. Schematic of the atomic force microscope setup.

2.4.3 Total Internal Reflection Microscopy

Total Internal Reflection Microscopy (TIRM) is another technique developed to measure colloidal interactions between a single microscopic sphere (3-30 μm in diameter) and a transparent flat plate; the assembly is immersed in a liquid. In this technique, the distance between the particle and the plate is monitored while the particle freely undergoes Brownian motions. Illuminating the particle by evanescent wave, the distance between the particle and the plate is calculated from the intensity of light scattered off the particle. From the equilibrium distribution of distances sampled by Brownian motions, the potential energy vs. distance relation can be determined. This technique covers a narrow range of force measurement compared to AFM or SFA [20, 23].

2.4.4 Micropipette Technique

The micropipette is a technique designed to study micron-scale objects, as illustrated in Figure 2.5. The method was originally developed in the field of biophysics to study blood cells and biological membranes [24, 25]; it was modified by Yeung and coworkers for applications in engineering science and oil sands research [26-31]. This technique will be used in this study to measure the *in situ* adhesive force of two micron-sized particles in non-polar solvent (i.e. hydrocarbon).

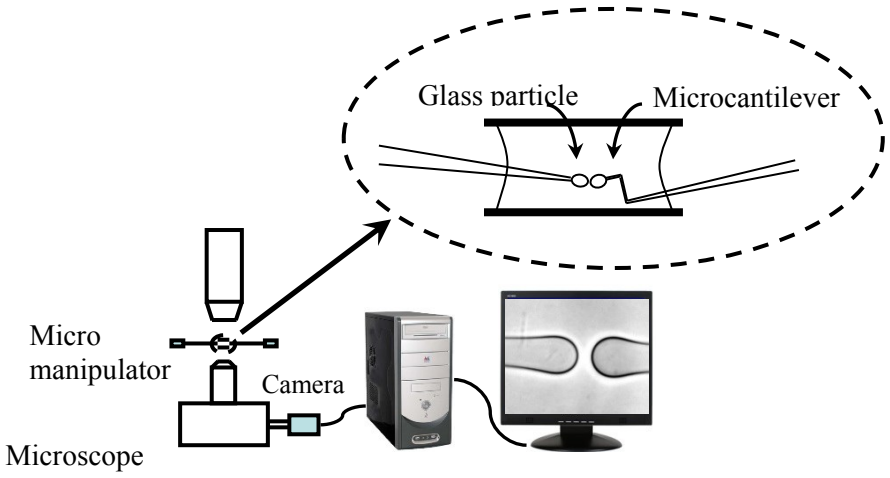

Figure 2.5. Schematic of the micropipette setup.

The measurement proceeds as follows: A small volume of hydrocarbon solution (approximately 200 μL) is placed in an open glass chamber and serves as the continuous phase. The glass chamber is made of two parallel cover slips with a 1 mm gap in between, as shown in Figure 2.6. To prevent unwanted evaporation of the volatile hydrocarbon, the chamber is completely immersed in water before the

oil phase was injected into the 1-mm gap; the solution is held inside the chamber simply by capillary forces. Next, two micropipettes are inserted into the two open sides of the chamber. These micropipettes, with round tips, would function as glass particles; the radii of curvature of the rounded tips are typically 10 μm (see photograph on monitor in Figure 2.5). Both pipettes are mounted on hydraulic micromanipulators (Narishige, model MHW-3) which enabled smooth 3-D motions of the tips inside the glass chamber. The colloidal interactions between the glass tips will be observed with an inverted microscope (Carl Zeiss Canada: Axiovert 200) that utilized transmission bright-field illumination. The microscope is connected to a camera and a computer. The video sequences are recorded digitally so that they can be analyzed after experimentation.

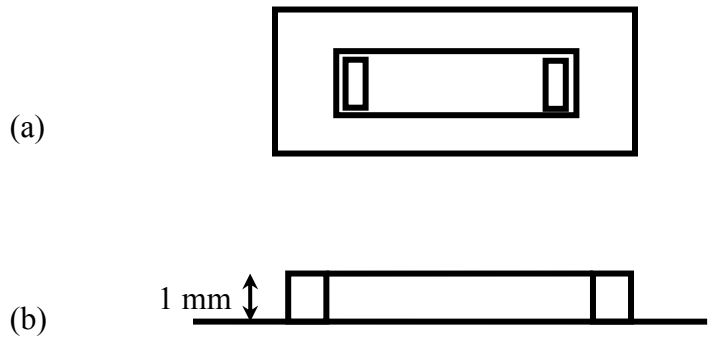

Figure 2.6. Schematic of the glass chamber used in micropipette experiments for holding liquid samples (~200 μL); the two sides of the chamber are open so that micropipettes can be inserted into the chamber. (a) Top view, (b) side view.

The micropipettes are prepared from glass capillary tubes with 1 mm outer diameter and 0.7 mm inner diameter (Kimble Glass Inc.). Individual capillary tubes are pulled along the axial direction at high temperature using a hot wire

pipette puller (David Kopf Instruments, model no. 730), resulting in two separate sections with tapered ends. (The sharp end of the taper is of submicron dimensions.) To produce a rounded end which mimics a spherical glass particle, the tips of the tapered pipettes were melted by bringing it close to a platinum hot wire. The resulting pipettes, with their rounded tips (Figure 2.7), will be used as glass particles in the experiment. Before experimentation, the melted tip pipette will be cleaned in mild sulphuric acid for 30 minutes and rinsed with de-ionised water.

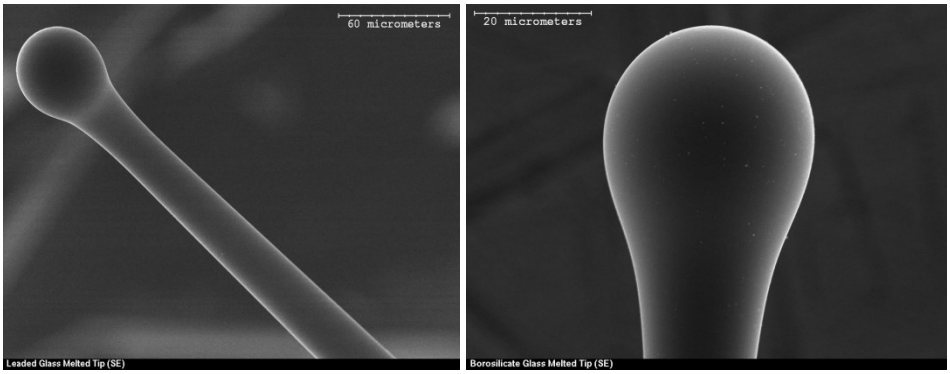

Figure 2.7. Melted tip of a micropipette used as glass particle in force measurement.

To produce a force-measuring device called the "micro-cantilever," one of the micropipettes is bent to right angles in two places, resulting in a periscope-like shape. The unique shape of the micro-cantilever gives the ability to measure adhesive forces between two solid spheres (i.e. the pipette tips). In particular, any axial force applied at the tip of a micro-cantilever will result in its deflection from the original position. The deflection of a micro-cantilever (Figure 2.8), which can be easily measured from microscope images, is directly proportional to its axial

load [31]. Knowing the Young's modulus of the pipette material (approximately 0.7×10^{11} Pa for borosilicate glass) and the detailed dimensions of the micro-cantilever, the cantilever stiffness k_b can be calculated based on beam theory.

With the above-mentioned capabilities, it is now possible to gently push the rounded tip of a straight micropipette against the tip of a micro-cantilever (while both pipettes are immersed in hydrocarbon) and measure the adhesive forces.

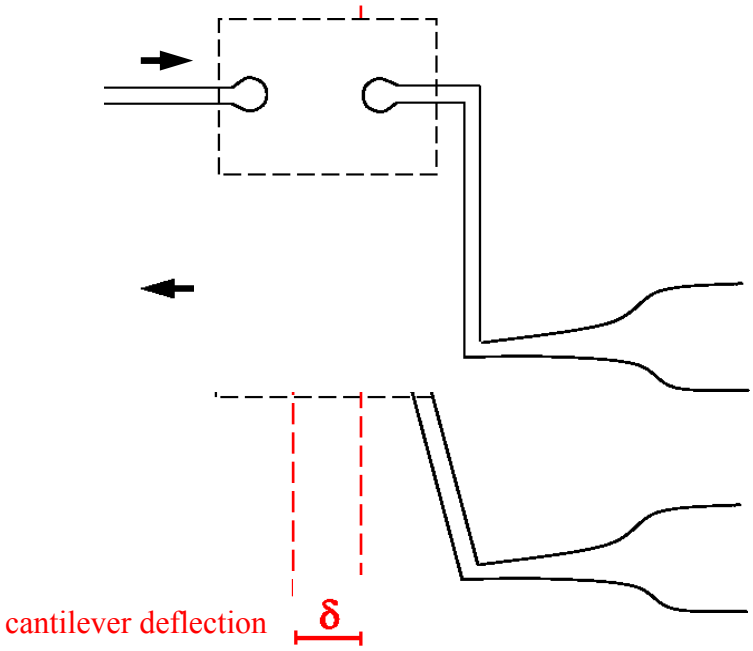

Figure 2.8. Sketch of the micro-cantilever experiment for determining the adhesive force between two pipette tips (functioning as glass particles). The cantilever on the right was kept stationary throughout the experiment.

The mentioned common techniques for direct surface force measurement such as SFA and AFM, have the advantage of detecting force versus distance and also measuring both adhesion and repulsion forces in both liquid and vapor systems.

However, as SFA works best with very smooth surfaces its application is limited to systems that match restricted material property of this device [20]. Also, cylindrical probes of SFA and planar geometry of counterpart sample in AFM result in geometry restriction of the samples.

In contrast, micropipette technique is a strong tool for inter-particle adhesive force measurements that does not have any limitation on the surface smoothness. Furthermore, it is capable of measuring forces in presence of bituminous material that reduce the clarity of the surrounding system. However, this technique can only detect adhesive force – in fact only the force of detachment.

2.5 Measurement of Surface Forces in Organic Liquids

There is a large body of literature on colloidal forces between solids and oil droplets in aqueous solutions using force measuring techniques [32-36]; however, much less attention has been devoted to non-aqueous systems. The force measurements that had been conducted in non-aqueous environments mainly focussed on the adsorption of polymers on different surfaces [37-40]. As a result, there are only a few studies on colloidal interactions of solids in non-aqueous systems.

Wang et al. (2009) studied the colloidal forces between silica surfaces coated with irreversible deposition of asphaltenes immersed in toluene; the work employed the AFM technique [41]. In their study, initially, a weak VDW attraction was detected between two bare silica surfaces immersed in toluene. Next, a silica

wafers and an 8-μm silica sphere were coated with an asphaltene layer. The thickness of the adsorbed layer was reported to be 3.5 nm for the flat coated surface, measured using AFM images. The force profile between an asphaltene-coated surface and a silica sphere surface, and that between two asphaltene films, are shown in Figure 2.9. Observed repulsive characteristics in these measurements indicated that VDW attraction was overcome by the strong steric repulsive forces created by the asphaltene tails and loops extended into toluene. The results also showed stronger repulsive forces as the two asphaltene layers become compressed.

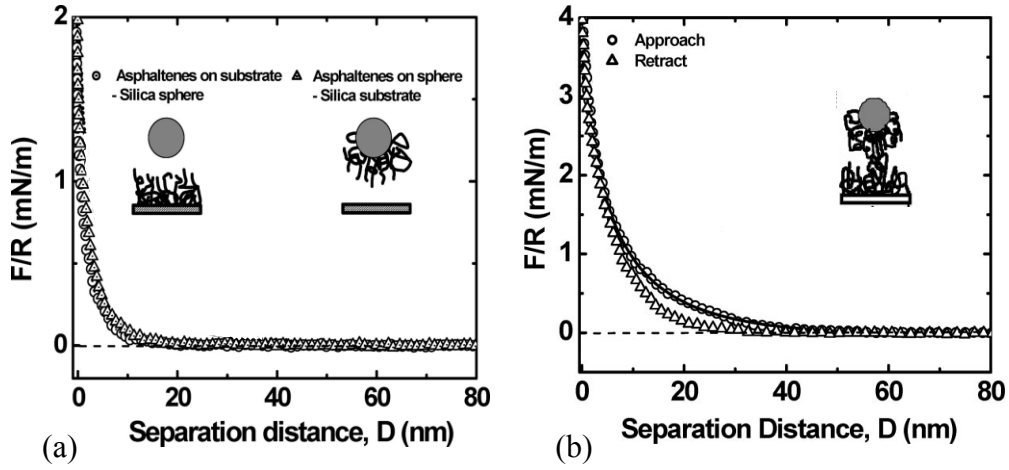

Figure 2.9. Normalized interaction forces between (a) asphaltene film and silica surfaces in toluene, and (b) two asphaltene films in toluene at 20°C.

Wang et al. (2010) extended the colloidal force measurement between the two asphaltene-coated surfaces in solvent consisting of different volume ratios of heptane to toluene (or 'heptol') mixture using AFM. The interaction between the asphaltene surfaces is shown in Figure 2.10(a), and the adhesion force as a

function of toluene content is shown in Figure 2.10(b). In pure toluene, Wang et al. observed steric repulsion between the surfaces. This steric repulsion is attributed to the polymer brush behaviour of swollen asphaltene chains adsorbed on the interacting surfaces (Figure 2.10(a)). Decreasing the toluene content in the system, adhesive forces were detected due to VDW interactions between asphaltene surfaces; the adhesive force was maximum in pure heptane [42]. Wang et al. did not investigate the effect of addition of bitumen material into the solvent system.

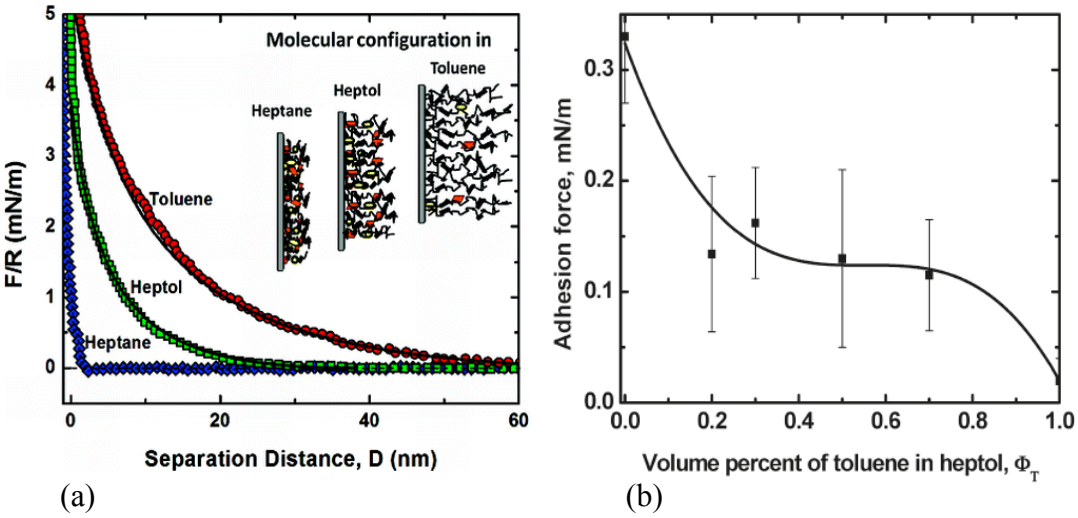

(a) (b)

Figure 2.10. (a) Interaction between asphaltene surfaces upon approach in heptol. (b) Adhesion force as a function of toluene volume fraction.

Natarajan et al. (2011) conducted similar force measurements between asphaltene-coated mica surfaces in toluene and heptane using SFA. They observed strong dependency of asphaltene surface interactions on solvent type, as well as contact time and pressure applied to the surfaces in the experiment.

Increasing the contact time and pressure on the coated surfaces affected mainly the results of force measurement in pure toluene [43]. They did not investigate the colloidal forces over the full range of toluene-heptane ratios.

Zahabi et al. (2010) studied the aggregation and settling of 1 μm asphaltene-coated silica particles over a range of pentane-toluene ratio, up to 0.5% (by weight). They observed that, by increasing the pentane content of the solvent (to over 33%), stable suspension of solids began to destabilize. They reported the onset of asphaltene precipitation (adsorbed on silica surfaces) to occur at a pentane to toluene ratio of 0.43 by weight; aggregation and sedimentation of particles increased dramatically above this ratio [19].

Zahabi et al. (2012) extended their study to the interaction forces between the asphaltene-coated gold substrate and the gold-coated AFM cantilever tip over the same range of pentane-toluene ratio. They detected very weak interactions in pure toluene (Figure 2.11). However, adhesion forces increased in higher pentane content and particularly over the onset of asphaltene precipitation (adsorbed on silica surfaces) [44].

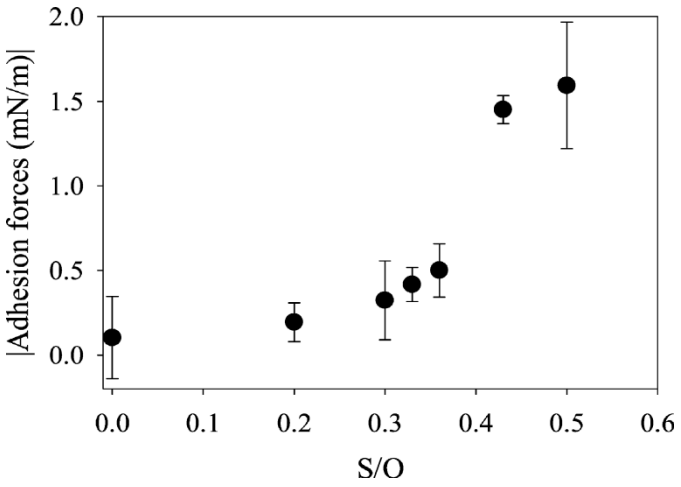

Figure 2.11. AFM adhesion forces for various pentane to toluene ratio by weight.

A similar investigation, but with a different experimental approach, had been carried out by Jin et al. (2011); it involved the colloidal interaction of bitumen-treated silica surfaces in non-aqueous media. Initially, the settling rates of pure and bitumen-coated silica particles (0.25 μm in diameter) were measured in toluene, *n*-heptane and heptol (i.e. a mixture of *n*-heptane and toluene); the results are shown in Figure 2.12.

(a)

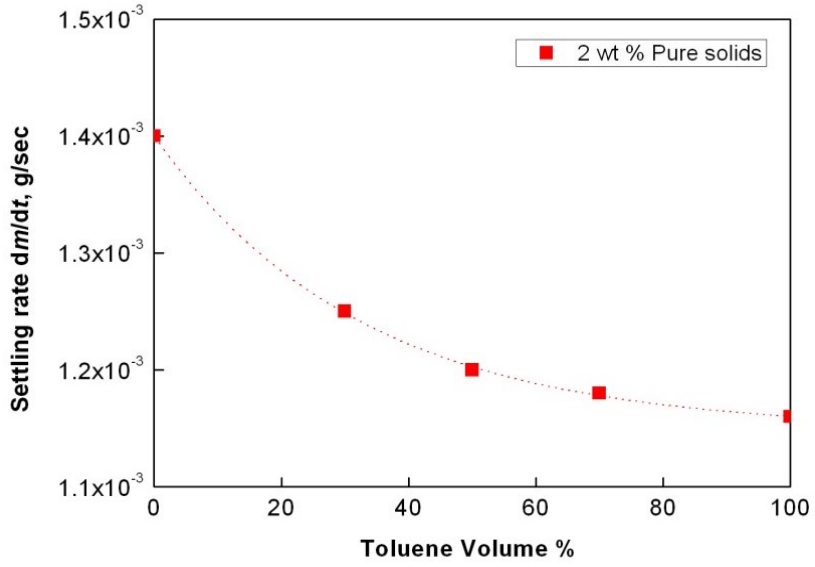

(b)

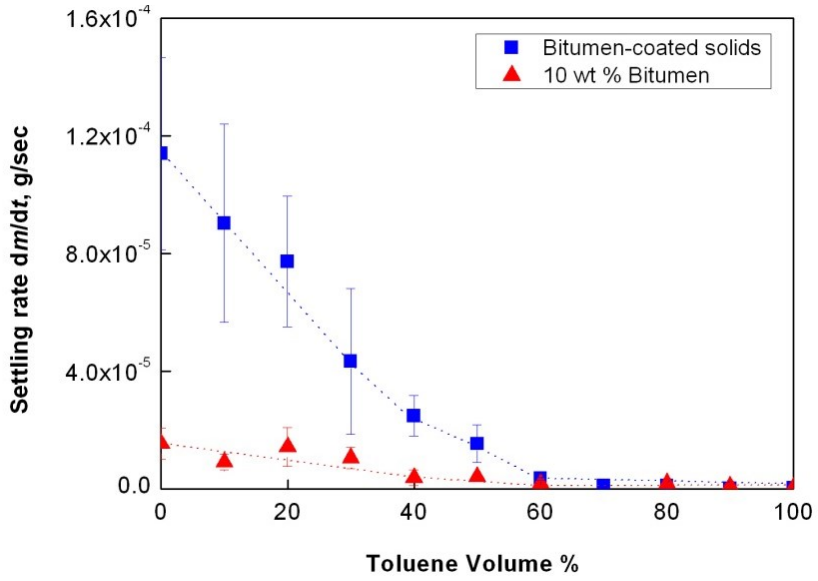

Figure 2.12. Settling rate of (a) clean silica particles in heptol, (b) bitumen-coated silica particles in heptol.

The results indicated that, as the solvent aromatic content increased, the settling rate dropped for both pure and coated particles. A similar trend was also observed by addition of bitumen to the solvent. This preliminary study was

complemented by micro-cantilever measurements of inter-particle forces, as shown in Figure 2.13.

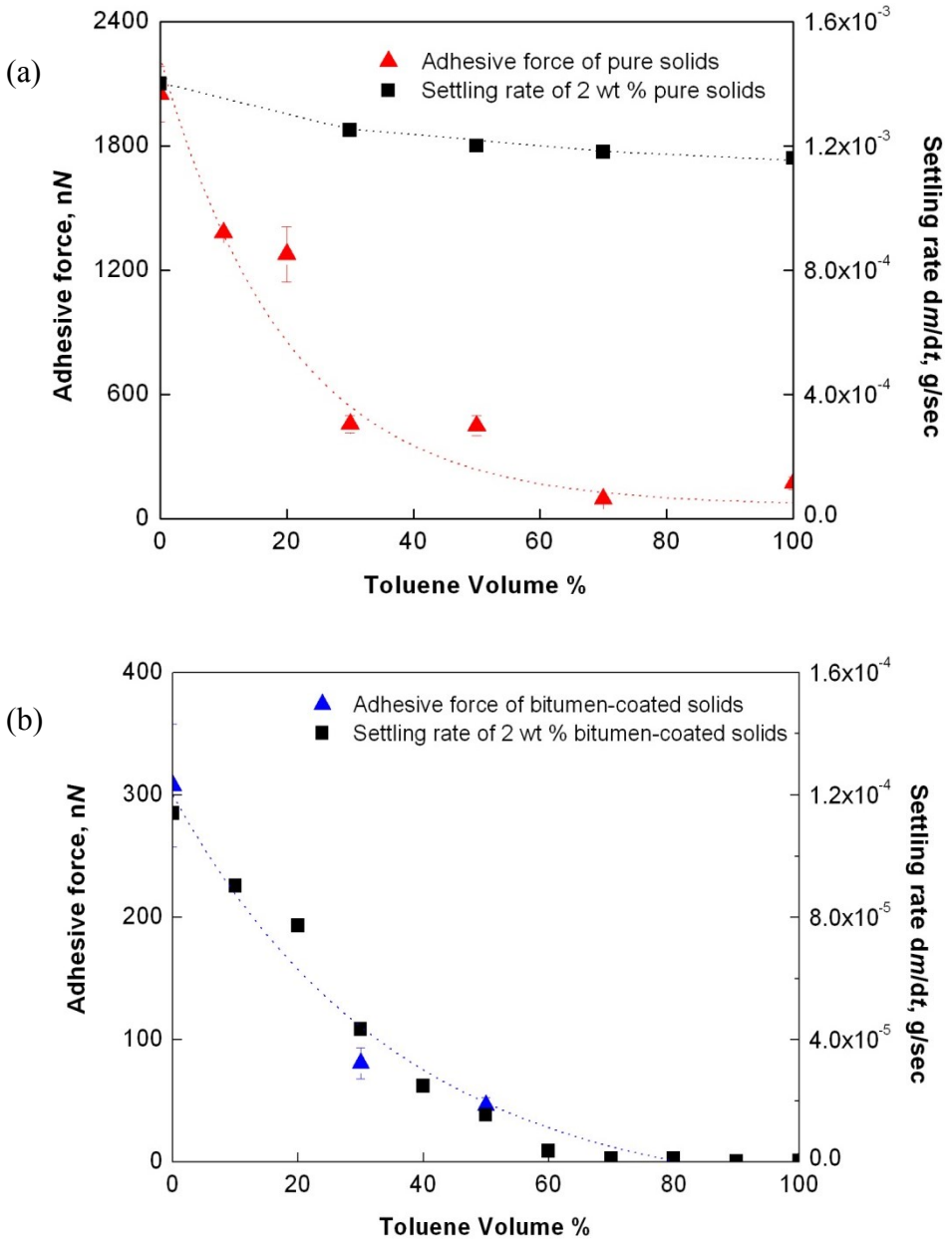

Figure 2.13. Simultaneous plots of settling rate and adhesive force as functions of solvent aromaticity. (a) Clean silica; (b) bitumen-coated silica.

They observed that the higher settling rates corresponded to stronger inter-particle forces for pure silica solids in toluene. Also, a strong increase in adhesive force was detected as the heptane content in the solvent was increased (Figure 2.12(a)). Moreover, for bitumen-coated particles, strong correlation was reported between the settling rates and particle-particle adhesion. (Figure 2.12(b)). Jin et al., however, did not study the effect of addition of bitumen to the suspending media.

2.6 Water-Soluble Surfactants in Bitumen

By nature, bitumen has surface active components that can modify the surface properties and enhance destabilization of solid particles in organic solvents. In this study, we propose addition of natural and synthetic surfactants to the system to enhance the wettability of the solid particles.

2.6.1 Surfactants

Surfactants are amphiphilic molecules consisting of a hydrophilic head group and a hydrophobic tail within the same molecular structure. These amphiphilic structures find their lowest energy states at the interfaces (e.g. oil-water interface) and prefer to be concentrated at such surfaces. Accumulation of surfactant at the interface results in interfacial tension (IFT) reduction. Most commonly, surfactants are categorized according to the type of their hydrophilic head groups. A non-ionic surfactant bears no charge in the head group. If the head group carries a negative charge, the surfactant is anionic and if the head group carries a positive charge, the surfactant is called cationic. The surfactant that contains both

positive and negative charges in the head group is called Zwitterionic or amphoterics. Surfactants tend to form spontaneous structures, called micelles, due to their amphiphilic nature. These self-assembled structures begin to appear at the critical micelle concentration (CMC). (At this point, decrease in IFT of the system stops.) Surfactants are mostly present at the oil-water interface, but they are also dissolved in the water and the oil phases. Some of them are more soluble in one of the phases.

2.6.2 Surfactants in Bitumen

Athabasca bitumen is a complex mixture of different chemical species. It is known that Athabasca bitumen contains natural ionic surfactants which mainly divide into three major types: surfactant with sulphonate ($-SO_3^-$) and sulphate ($-OSO_3^-$) head groups, carboxylic acid group (-COOH), and various types of amines ($-NH_2$) [45, 46].

Naphthenic acids (NA), which is a class of carboxylic surfactants, forms the largest fraction of surfactants indigenous to Athabasca bitumen with an abundance of 1-2 wt%. NA is a mixture of mono- and poly-cycloalkane carboxylic acids with aeliphatic side chains of various lengths [47]. Due to the very favourable interfacial properties of naphthenic acids, namely, its ability to significantly reduce the oil-water interfacial tension and render the solid substrate hydrophilic, the surfactant is of interest in this study. Naphthenic acids can be extracted from bitumen by addition of an alkaline solution to bitumen. In the

extraction process, naphthenic acids are converted into water-soluble sodium naphthenates (SN) [48, 49].

3. Experimental

3.1 Preparation of Solids Free Bitumen

The bitumen used in this research was the residue of the diluent recovery unit (so-called "DRU bottoms") obtained from Syncrude Canada Ltd. The bitumen sample was treated to remove any submicron clay particles prior to all experiments. To remove the clays, bitumen was diluted in toluene at a 1:1 mass ratio; the solution was then centrifuged at 35,000 g (Thermo Electron Corporation, model RC 6 Plus) for 2 hours [50]. Based on Stokes' law, particles as small as ~10 nm would be removed. Following centrifugation, a rotary evaporator (BÜCHI, model no. R200) was used to remove toluene from the "solids free" supernatant at 45°C for 1 hour. After that, the solids free solution (now with most of the toluene evaporated) was placed under the fume hood for several days in order to remove the residual toluene; the procedure was considered complete when the original bitumen mass was recovered.

3.2 Preparation of De-Asphalted Bitumen

The solids-free bitumen was either used directly in the experiments, or further treated to remove asphaltenes. The solids-free and asphaltene-free bitumen was referred to as de-asphalted bitumen or maltene. To remove asphaltenes, *n*-heptane was added to bitumen at a volume ratio of 40:1 (40 parts *n*-heptane + 1 part bitumen). The mixture was agitated for 2 hours in a shaking incubator

(JeioTech, SI-600) and aged for 24 hours. A vacuum filter (Fisher Scientific, 47 mm all-glass vacuum filter holder) was used to separate the precipitated asphaltenes from the aged mixture using 0.22-μm pore-size filter papers. The *n*-heptane was removed from the filtrate using a rotary evaporator. To remove the remaining asphaltenes from bitumen, the residue from the rotary evaporator was mixed with *n*-heptane at a volume ratio of 4:1 (4 parts *n*-heptane + 1 part bitumen), followed by the same shaking, aging, filtration and evaporation procedure.

3.3 Preparation of Silica Beads

Spherical silica particles, 1 μm in diameter, were purchased from Fiber Optic Center Inc. The factory received beads were heated in a muffle furnace (Thermoscientific Thermolyne heavy duty muffle furnace, model FA1730) at 650ºC for 2 hours to remove any possible chemical residue on the surface. Prior to sedimentation tests, the silica particles were treated in a toluene-diluted bitumen solution (1 part bitumen + 4 part toluene) for 1 hour. The particles were then washed multiple times with fresh toluene to ensure that only the irreversibly adsorbed bituminous material remained on the surface of the particles. Next, the particles were recovered by centrifuging the mixture (Beckman, model JA-10). The bitumen-treated silica particles were dried in a fume hood for 2 days and stored in sealed opaque bottles.

Silica particles that have been bitumen-treated are assumed to closely mimic the indigenous fine particles in oil sand ores. The X-ray photoelectron spectroscopy (XPS) of the clean and bitumen-treated flat silica substrate is reported in Table 3.1. The thickness of the adsorbed layer was detected to be 8 nm on the flat coated surface.

Table 3.1. Elemental analysis of clean and bitumen-treated silica substrates by X-ray photoelectron spectroscopy.

elements	mass concentration %	
	clean	Bitumen-treated
O	47.98	41.46
N	0.35	0.49
C	18.34	27.06
S	0.06	1.45
Si	33.25	29.51

3.4 Materials

3.4.1 Aqueous Phase

The aqueous (dispersed) phase was de-ionised water prepared by Millipore (Milli-Q Advantage A10 Ultrapure Water Purification System).

3.4.2 Surfactants

The surfactant-water solution was formed by dissolving different concentrations of surfactants into de-ionised distilled water (DI water). In this study, four types of surfactants were used which included both cationic and anionic surfactants. The first three surfactants were cetrimonium bromide (CTAB), sodium dodecylsulfate (SDS), and sodium dodecylbenzenesulfonate (SDBS); they were

supplied by Sigma-Aldrich. The fourth surfactant was sodium naphthenates (SN) supplied by Eastman Kodak (practical grade); it was used as received without further purification.

SDS was chosen as a commercially available surfactant. In contrast to the other three surfactants, CTAB is a cationic surfactant. SDBS molecular structure contains an aromatic ring which gives a relative similarity to some of the compounds available in bitumen. Finally SN was chosen due to very favourable interfacial properties and also its natural abundance in bitumen. Combination of these properties covers a wide range of surfactants for this research.

3.4.3 Hydrocarbon Phase

The oil phase consisted of pure solvents of variable toluene-to-heptane ratios (the so-called "heptol" mixtures). As the experiments went further, bitumen and maltene (i.e. de-asphalted bitumen) were also added to the heptol. Toluene and *n*-heptane (both HPLC grade) were purchased from Fisher Scientific Canada.

3.5 Sedimentation of Silica Particles

The settling behavior of treated silica particles was studied in different hydrocarbon environments; this constituted a systematic examination of inter-particle interactions. The experiments were initially conducted in different volume ratios of heptane to toluene (heptol) mixtures with 5 wt% solids. The suspension was contained in a PTFE (i.e. Teflon®) bottle and agitated in a water bath sonicator (Transonic 310) for 5 minutes to ensure adequate mixing and

dispersion. In later tests, maltene or full bitumen were added to the heptol mixtures to a concentration of 3wt% maltene or 4.5wt% bitumen.

In this study, the settling rate of particles was tracked using a sedimentation balance (KRÜSS K100). This device consists of a platinum tray which is attached to a balance. The tray is submerged in the suspension at a predetermined distance below the liquid surface. A sketch of the experimental setup is shown in Figure 3.1a. As the particles settle, the mass of solids collected on the tray increases over time. The weight change of the tray, recorded by a microbalance, gives an accurate measure of the mass of solids (m) as time (t) progresses. A typical plot of the solids mass m vs time t is shown in Figure 3.1b. The start time is defined as the moment when sonication of the mixture ceases and the solids are allowed to settle under gravity. After a certain time period, the mass of solids collected on the tray reaches a plateau. This is the time required for the solid particles in the liquid column above the tray to completely settle onto the tray. For the purpose of this study, this time will be called the "settling time," and the inverse of the settling time will be used as a measure of the particle settling rate. In essence, the settling rate defined in this manner shows the rate of normalized mass fractions rather than the absolute mass (i.e. settling rate = $\frac{dm}{dt} \times \frac{1}{m}$, where m is the total mass collected over infinite time). Therefore, on the sedimentation curve shown in Figure 3.1b, the settling rate is not measured by the slope of the curve, but by the settling time. The shorter the settling time, the faster the settling rate.

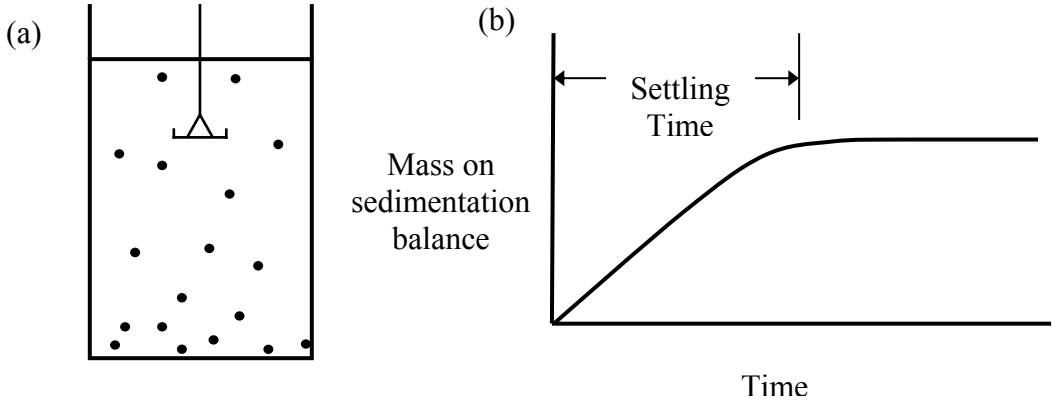

Figure 3.1. (a) Schematic of the sedimentation experiment; (b) a typical plot of the solids mass m vs time t generated from the sedimentation experiment.

3.6 Inter-Particle Adhesion Force

Inter-particle forces play a central role in the aggregation or dispersion of silica particles in the hydrocarbon medium. The most accurate way of examining colloidal interactions in oil media is through direct measurement of inter-particle forces. Thus, in the next parts of this study, a novel micromechanical technique was used to measure the inter-particle adhesion force. In this method, the rounded tips of a glass micropipette and micro-cantilever act as the solid particles. Due to similar properties of glass and silica, the rounded tip of a micropipette can approximate a silica surface. These tips have been pre-treated in toluene-diluted bitumen solution for more than 1 hour; this procedure allows sufficient time for the deposition/adsorption of bitumen material onto the glass surfaces and create bitumen-coated "particles."

To measure the adhesive inter-particle force, the tip of one micropipette was manipulated into contact with the tip of a micro-cantilever under a microscope. The entire system was suspended in the hydrocarbon phase. Once the tips were in contact, the micropipette was pulled back. Because of the adhesion force between the surfaces, the cantilever tip will be attracted to the micropipette tip and would deflect it from its original position. The deflection of the micro-cantilever δ is directly proportional to its axial load [31]. Knowing the Young's modulus of the pipette and the dimensions of the micro-cantilever, the elastic stiffness k_{b} can be calculated based on beam theory. Details of the cantilever stiffness calculations can be found in Appendix B. With the cantilever behaving as a linear spring, it is possible to calculate the adhesion force from the following relation:

$$F = k_{\mathrm{b}}\,\delta \qquad \text{Equation 3.1}$$

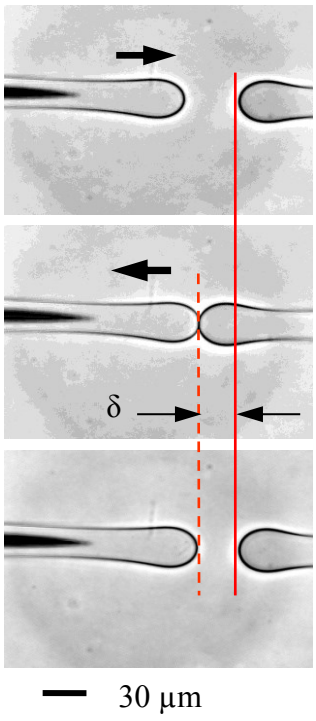

Figure 3.2. Actual microscope images of a force-measuring experiment between two rounded pipette tips (which function as glass beads). The cantilever pipette on the right was kept stationary throughout; its only motion was its deflection as the pipette on the left was pulled back. The cantilever deflection δ provided a direct measure of the adhesive force.

3.7 Water-Particle Adhesion Force

To determine the adhesive force between a water drop and a solid particle (immersed in hydrocarbon), a micropipette, with an inner diameter of about 60 µm, is filled with the aqueous phase. This pipette is directly connected to a syringe pump to apply adjustable pressure. The whole set up (i.e. micro-cantilever and the larger, water-filled pipette) is then immersed into the oil phase.

Once the rounded glass tip of the microcantilever is placed just inside the large pipette (top photo in Figure 3.3), the pressure in the pipette is slowly increased until the aqueous phase makes contact with the glass tip. Next, the aqueous phase in the pipette is slowly pulled back. If there is any adhesive force between the glass particle and the aqueous phase, the cantilever will deflect from its original position; this deflection is proportional to the adhesive force [31]. Knowing the cantilever stiffness (as discussed in Section 3.3) and also its deflection, it is easy to calculate the adhesive force from Hooke's law.

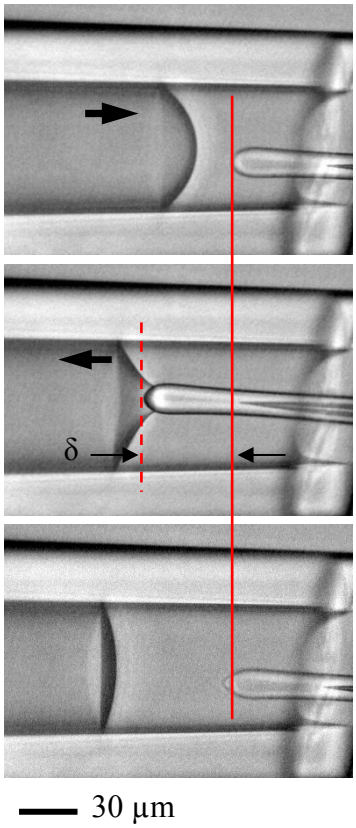

Figure 3.3. Actual microscope images of a force-measuring experiment between the pipette tip (which functions as a glass bead) and water. The cantilever pipette on the right was kept stationary throughout, while the water inside the pipette (on

the left hand side) was moved. The cantilever deflection δ provided a direct measure of the adhesive force.

3.8 Interfacial Tension (IFT) Measurement

The micropipette technique is capable of quantifying normal to very low interfacial tensions (~10^{-4} mN/m). One of the main advantages in using micropipettes is the in situ measurements on the pore scale [51, 52]. In this method, a micropipette (with inner radius of ~10 μm) filled with an aqueous phase is immersed into the oil. The aqueous phase is then pushed out of the pipette tip very slowly by increasing the pressure in the pipette. The change in pipette pressure is controlled either through a syringe connected directly to the pipette (suitable for IFTs of order 1 to 10^2 mN/m), or by adjusting the elevation of a water reservoir — and hence the hydrostatic pressure at the pipette tip (suitable for IFTs ranging from 10^{-4} to 1 mN/m). The minimum pressure necessary to expel water from the pipette tip is related to the oil-water interfacial tension (IFT) through the Young-Laplace equation

$$\Delta p = \frac{2\gamma}{R_{\mathrm{p}}} \qquad \text{Equation 3.2}$$

where Δp (Pa) is the pressure to expel water from the pipette, γ (N/m) is the interfacial tension, and R_{p} (m) is the inner radius of the pipette.

4. Results and Discussions

As mentioned earlier, one of the main challenges to the solvent-based extraction process is removal of fine solids that are suspended in non-aqueous media. These fine clays and colloidal silica that remain can range from the submicron scale (~10 nm) to several microns. The fine solids cannot be removed through usual methods of separation. However, there are mechanisms that cause these particles to destabilize and form aggregates; removal of the aggregates is then possible through various separation methods. Two of these mechanisms by which the small particles can be destabilized are: homo-aggregation (i.e. adhesion between the solid particles) and hetero-aggregation (i.e. the use of emulsified water as 'collectors') of the solids.

Homo-aggregation is the aggregation of the particulates amongst themselves. A sketch of this mechanism is shown in Figure 4.1(a). Aggregation of the particles leads to formation of 'flocs' (with increase in effective size) that now can be separated through centrifugation or gravity settling. Note that these aggregations occur in non-aqueous liquids (i.e. solvent-diluted bitumen); as mentioned earlier (section 2.3), non-aqueous colloidal interactions are not studied nearly as much as its aqueous counterpart.

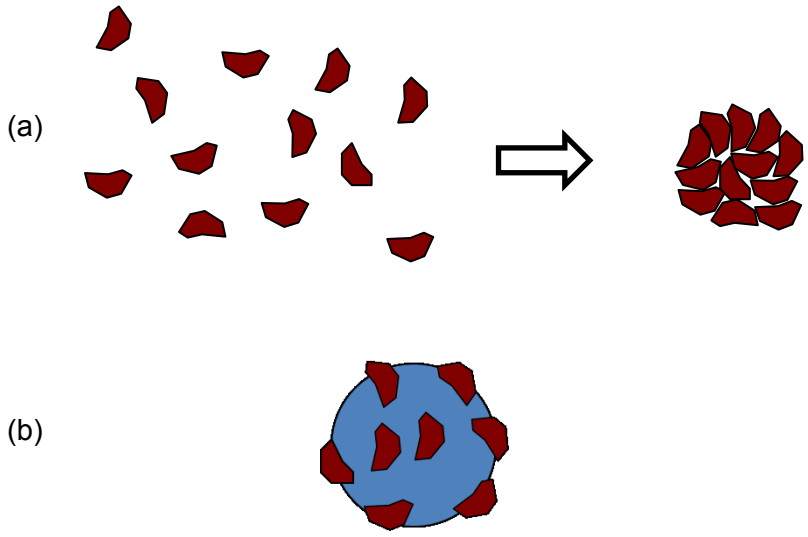

Figure 4.1. Two mechanisms of gathering fine solids in a hydrocarbon environment: (a) by homo-aggregation, and (b) using water droplets as "collectors."

Fine particulates can also be trapped at fluid-fluid interfaces by surface tension forces. Therefore, manipulating the surface properties of the particulates can be very helpful to their collection and subsequent removal. Introducing small amounts of emulsified water deliberately into the oil phase can create oil-water interfaces which function as "particle traps" and lead to hetero-aggregation of solids. Moreover, it may be possible to customize the chemistry and composition of the aqueous phase (e.g. with addition of water-soluble surfactants) to facilitate particle capture; under very favourable conditions, this may even result in the transport of particulates across the oil-water interface and into the aqueous phase. A sketch of particle capture by water droplets is illustrated in Figure 4.1(b). In the following sections, each mechanism of solids capture is investigated in details.

4.1 Homo-Aggregation of Solids

In this section, our goal is to investigate the homo-aggregation of solids in organic solvents. This was accomplished through bench scale sedimentation experiments to determine the settling rate of silica particles in organic solvents with different degrees of aromatic content. The sedimentation experiments were then followed by measurements of adhesive forces between silica particles using the micro-cantilever technique. The experiments were initially conducted in an oil phase of diluted maltene (i.e. diluted de-asphalted bitumen) to eliminate the influence of asphaltene precipitation on particle interactions. This was followed by the replacement of maltene with actual bitumen in the system to determine the impact of asphaltene precipitation on inter-particle interactions.

4.1.1 Settling Tests

The settling of bitumen-treated silica was initially investigated in pure heptol (i.e. 0 wt% bitumen); the results are shown in Figure 4.2. In this graph, the horizontal axis represents the amount of toluene (in vol%) contained in the heptol mixture, and the vertical axis is the normalized settling rate of solid particles (see Section 3.5). The results show that in pure heptol, the settling rate of the particles depends strongly on the aromatic content in the heptol: at higher toluene contents (i.e. higher aromatic content), the settling rates were lower, suggesting increased colloidal stability of the silica particles. Note that experimental data for heptol containing less than 50 vol% toluene could not be obtained because of the high

affinity of the silica particles to all objects: in addition to adhering with one another, which was what we had expected, the particles were deposited also onto the shaft and the bottom of the sedimentation dish (see Figure 3.1a), rendering the registered mass meaningless. This observed phenomenon will be discussed further in the next section. The dashed blue line in Figure 4.2 represents only the *expected* settling rates of bitumen-treated silica in pure heptol at low aromatic contents.

In the next step, the simple case of bitumen-coated silica settling in heptol (blue line in Figure 4.2) was modified to a more realistic situation: by adding 3wt% maltene to the heptol solvent. The settling results are also presented in Figure 4.2 red line). In the presence of maltene, the settling rates of silica particles showed the same qualitative dependency on the solvent's aromatic content. Quantitatively, however, the addition of maltene to the system leads to an overall

decrease in the settling rates.

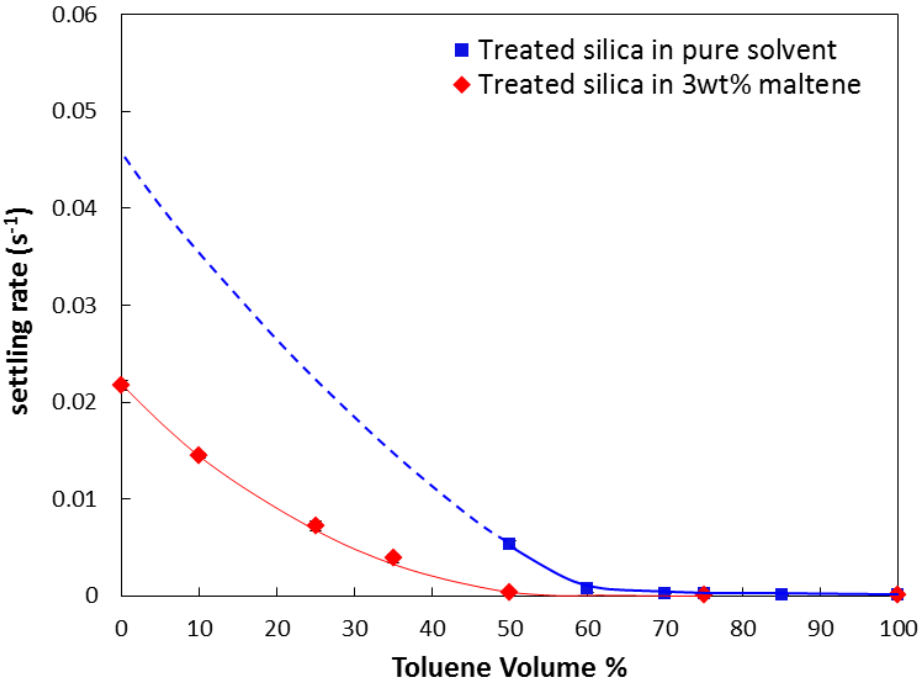

Figure 4.2. Settling rate of bitumen-treated silica in pure heptol (in blue) and heptol + 3 wt% maltene (red). Recall "heptol" is an organic solvent which is a mixture of toluene and *n*-heptane. The dotted blue line represents the expected settling rates below 50 vol% toluene in heptol.

As shown in Figure 4.2, for pure heptol with more than 70 vol% toluene, the settling rate of the silica particles was very low (on the order of 10^{-4} s^{-1}) and could effectively be considered zero. With the addition of 3wt% maltene, the point of "zero" settling rate was shifted to a lower toluene content — to about 50 vol% toluene.

In contrast, the observed non-zero settling rates at low toluene contents could be a consequence of significant aggregation of the 1-µm silica particles. To test such a hypothesis, the micro-cantilever technique was used to measure inter-particle

forces between bitumen-treated glass particles (diameters of approx. 30 μm) in both pure heptol and heptol with 3 wt% maltene.

4.1.2 Adhesive Force Measurements

The adhesive force between two bitumen-coated particles, measured by the micro-cantilever technique, is shown in Figure 4.3. As seen, the adhesive force is directly related to the toluene volume ratio in heptol, and it dramatically increases as the toluene content decreases. This explains the strong attachment of particles to each other and to the balance shaft when the toluene content was lower than 50 vol% (or equivalently, when the *n*-heptane content was higher than 50 vol%). Although the measured forces in the presence of maltene showed weaker adhesion compared to in pure heptol, these forces are still strong enough for the particles to homo-aggregate and settle at higher *n*-heptane contents.

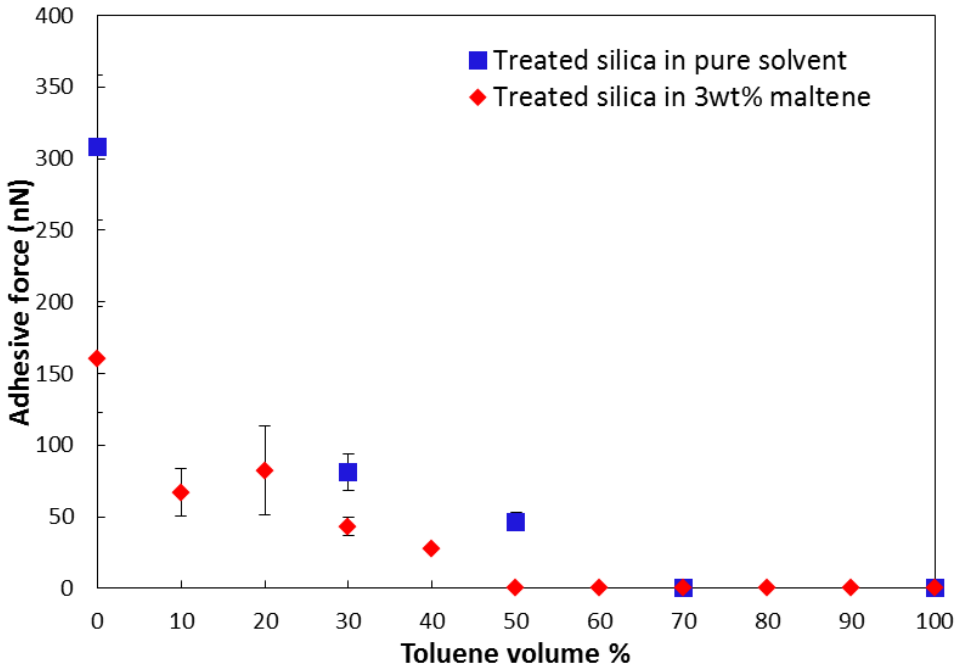

Figure 4.3. Adhesive force between bitumen-treated glass spheres in pure heptol (blue symbols) and heptol + 3 wt% maltene (red symbols). The forces were measured by the microcantilever technique.

As seen in Figure 4.2 and Figure 4.3, when there was very little or no aromatic solvent in heptol, the silica particles aggregated strongly with one another (i.e. they homo-aggregated) and settled rapidly. This strong inter-particle interaction and fast settling, however, decreased with increasing toluene content in the system. Also, the addition of maltene to heptol caused a shift in both zero force and zero settling rate — from 70 vol% toluene in pure heptol to 50 vol% toluene in the presence of maltene. The striking similarities between Figure 4.2 and Figure 4.3 suggest a strong correlation between the rate of particle sedimentation and inter-particle forces. This correlation is strong evidence for homo-aggregation of the silica particles in the absence of asphaltene molecules. In an

earlier study in our group, Jin et al. (2011) suggested that the adhesive force between bitumen-treated particles in heptol was due fundamentally to van der Waals interactions [15]. If the adsorbed layer of bitumen on the silica surface acted like asphaltene, it will swell and form a brush-like steric barrier in toluene (the 'good solvent'), thus preventing the particles from aggregating. By substituting toluene with heptane, the adsorbed asphaltene layer will likely collapse onto the surface and hence allow two particles to approach closer to one another. In this situation, the van der Waals attraction between particles comes into effect. A schematic of this phenomenon is shown in Figure 4.4. According to the above hypothesis, the aromatic content of the solvent should have strong effects on the magnitude of the inter-particle forces; this is in agreement with the force measurement results and the sedimentation behavior presented in Figure 4.2 and Figure 4.3.

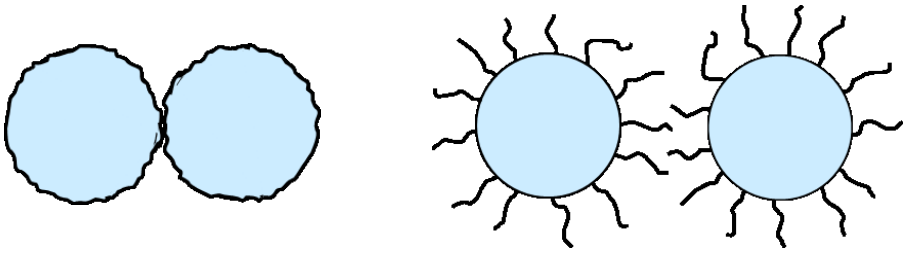

Figure 4.4. Bitumen-treated solid particles in a paraffinic solvent (the "poor" solvent) and an aromatic solvent (the "good" solvent). These scenarios, if true, would imply that the adsorbed materials are "asphaltene-like."

The van der Waals force between two identical spheres can be calculated using the Derjaguin's approximation:

$$F_{\mathrm{vdW}} = -\frac{A_{\mathrm{eff}} R}{12 D^2} \qquad \text{Equation 4.1}$$

where D is the separation distance between the two spheres, A_{eff} is the effective Hamaker constant of the system, and R is the radius of sphere [20].

In pure *n*-heptane, when the detected force is strongest (~300 nN measured with cantilever technique in Figure 4.3), the vdW force between the coated solids can be calculated by using the effective Hamaker constant of 1.1×10^{-21} J [42, 53]. Setting the separation distance *D* as 1 nm, the calculated force is two order of magnitude smaller than what is detected using the cantilever technique. We took another approach and calculated *D* based on the experimental force value (300 nN); the separation distance is 0.05 nm which is unrealistic. Either way, the conclusion is that there must be other additional contributions to the adhesive force. In practice, when the two bitumen-treated surfaces are detaching, the measured force is a combination of the vdW force and an additional interaction originating from the entanglement of the asphaltene- like molecules adsorbed on the solid surfaces. Therefore, the measured force is larger than the VDW force alone.

As maltene was introduced into the solvent, a general decrease in the measured forces was observed. Taylor et al. (2001) reported an increase in refractive index of the solvent as a result of the addition of maltene to hydrocarbons [54]. It is

plausible that this phenomenon will decrease the Hamaker constant and therefore the resulting vdW force. At the same time, we speculate that the presence of maltene molecules will increase the separation distance (i.e. D) between two particles, hence also lowering the van der Waals force. Therefore, the addition of maltene to the system will change both the Hamaker constant and separation distance simultaneously. This hypothesis explains the general decrease in measured forces upon the addition of maltene and also the shift in effective zero force from 70 vol% to 50 vol% toluene content in the presence of maltene (Figure 4.2).

4.1.3 Insights into the Paraffinic Froth Treatment Process

The mentioned experiments to this point, however, are somewhat artificial as they were carried out in the absence of asphaltene precipitation. A more realistic scenario would be for the bitumen-treated silica to settle in diluted bitumen. If bitumen were diluted with a paraffinic solvent, the underlying dynamics would resemble those of a "paraffinic froth treatment" or PFT process (discussed in Section 1.3). When mixed with a paraffinic solvent such as *n*-heptane, the two components of bitumen — maltene and asphaltene — will manifest themselves as follows:

- The maltenes will be dissolved (by definition), forming a solution which we call "diluted maltene."

- The asphaltenes will first nucleate as small "primary particles" that are distributed throughout the suspending medium (the diluted maltene). As these particles collide and adhere to one another, they form loose networks and begin to settle. Provided that no mechanical agitation is applied, the dominant mechanism of inter-particle collision is differential settling (i.e. larger aggregates, with their faster settling velocities, catch up to smaller aggregates and make contact). Differential settling is a "self-amplifying" effect which can significantly shorten the sedimentation time of colloidal particles, often by orders of magnitude.

The focus of this study, however, is not on asphaltene precipitation; it is on the sedimentation and separation of colloidal silica (or any other type of inorganic solids) in diluted bitumen. For simplicity, we focus only on situations where the diluting solvent is *n*-heptane (i.e. heptol with 0% toluene). In such cases, the settling of inorganic solids would occur concurrently with the precipitation/sedimentation of asphaltenes. The central question is: how will precipitation of asphaltenes affect the homo-aggregation of silica? In the investigation which follows, we will use settling rate (described in Section 3.5) as an indicator of aggregation and sedimentation. (Due to the opacity of crude oil and the obstruction of asphaltene precipitates, direct microscopic observation is not possible.) Also, for reasons that will be explained later, we will begin our sedimentation balance measurements at a shallow depth of 1.5 cm.

We begin by comparing the settling rates of (A) silica alone, and (B) asphaltenes alone — both in diluted maltene solutions of the same maltene content. The settling of silica in 3 wt% diluted maltene is shown by Curve A of Figure 4.5; the corresponding settling rate is 0.022 s^{-1} (the same rate as shown in Figure 4.2 for 0% toluene). Next, the settling of precipitated asphaltenes in 4.5 wt% diluted bitumen is depicted by Curve B of the same figure. (Reason for choosing such a concentration: 4.5 wt% diluted bitumen $\cong$ 3 wt% diluted maltene + precipitated asphaltenes.) In this case, the settling rate was 0.0035 s^{-1} — approximately seven times slower than that for silica in 3 wt% diluted maltene. Cases A and B were control tests whose results are needed for comparative purposes. The next case to be tested, Case C, would address the crucial question of how precipitated asphaltenes affect the homo-aggregation of inorganic solids. This case involved the sedimentation of silica in 4.5 wt% diluted bitumen; this, we reasoned, was equivalent to the settling of silica particles + precipitated asphaltenes, all in 3 wt% diluted maltene. The settling curve for Case C is shown also in Figure 4.5. Interpretations of this curve proceed as follows:

- We first note that the steady state mass of Curve C (the plateau value) is the sum of the steady state masses from Curves A and B. This "mass balance" is very significant: it suggests that all silica particles in Case C settled in an "accelerated" manner — either through homo-aggregation amongst themselves, or hetero-aggregation with the asphaltene networks. Free silica particles, with a diameter of 1 μm, would effectively be

"neutrally buoyant" on time scales relevant to Figure 4.5; as such, they would not be detected by the sedimentation balance. If any appreciable amount of colloidal silica were discrete (i.e. non-aggregated) particles, we would not have the observed mass balance.

- It is seen from Figure 4.5 that the settling rate in Case C was practically the same as that for Case B (involving only asphaltene networks); this is another very important observation: From the apparent mass balance, we had deduced that all silica particles in Case C either participated in homo-aggregation or were captured by the asphaltene networks. Yet, if silica homo-aggregation did occur, even for only a fraction of the silica, the resulting settling rate would be some intermediate value between 0.022 s^{-1} (Case A) and 0.0035 s^{-1} (Case B). The fact that Case C's settling rate is at the lower limit implies that no significant homo-aggregation had occurred.

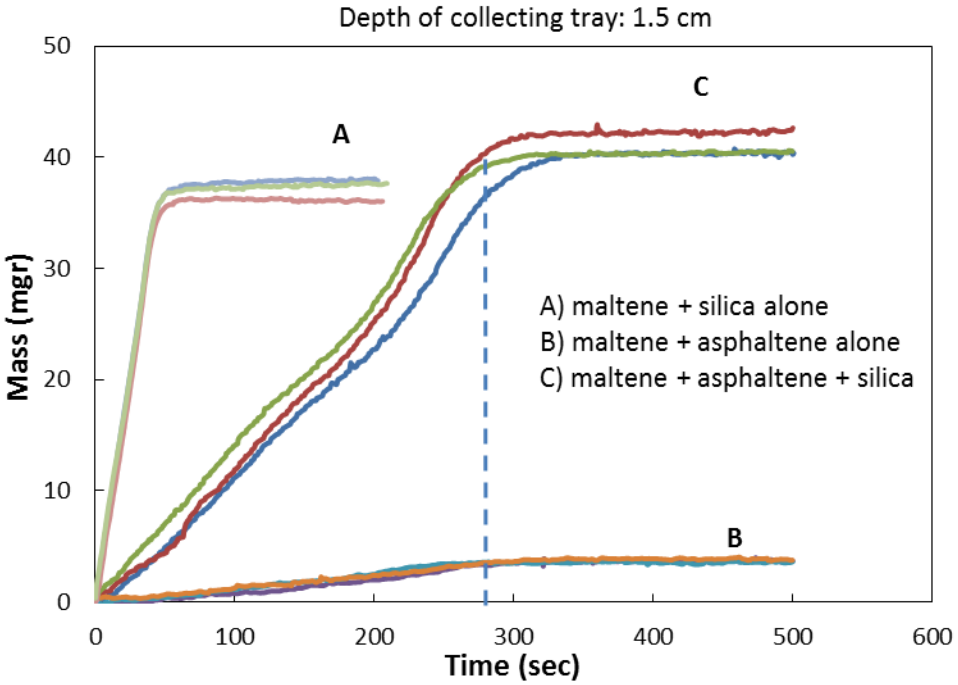

Figure 4.5. The settling curve for (A) bitumen-treated silica particles in 3 wt% diluted maltene, (B) precipitated asphaltenes in 4.5 wt% diluted bitumen (no silica particles), and (C) bitumen-treated silica particles in 4.5 wt% diluted bitumen. The collecting tray was located at depth of 1.5 cm.

Based on the above "shallow depth" observations, we can draw two very important conclusions: (1) asphaltene precipitation suppresses the homo-aggregation of bitumen-treated silica particles, possibly through formation of steric barriers at the particle surfaces, and (2) all stabilized solids are captured by the asphaltene networks and settle as asphaltene-silica complexes.

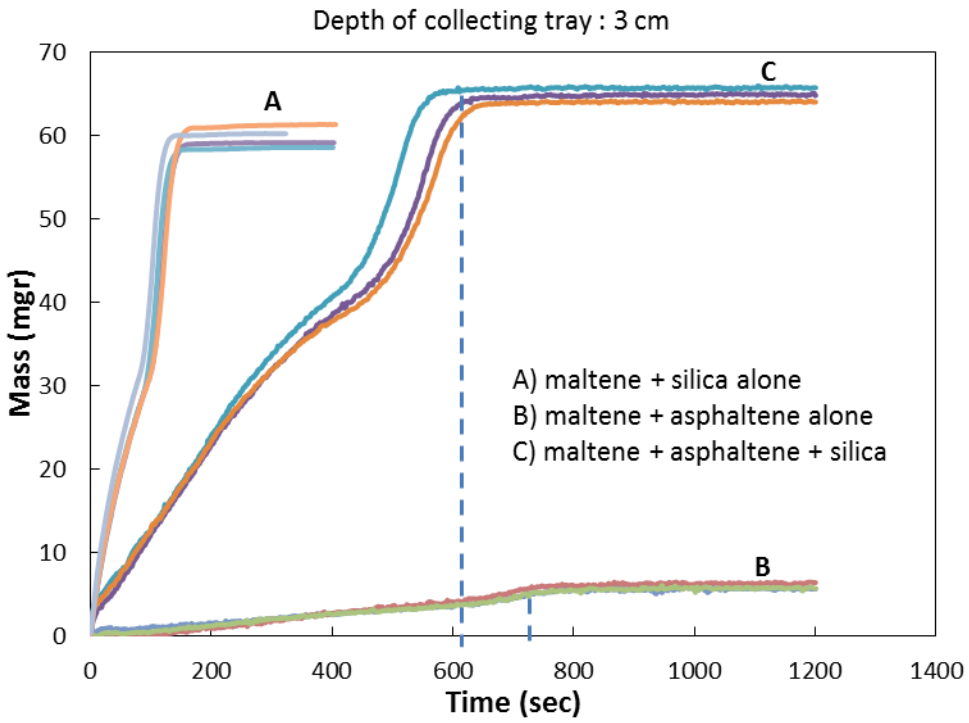

Figure 4.6. The settling curve for (A) bitumen-treated silica particles in 3 wt% diluted maltene, (B) precipitated asphaltenes in 4.5 wt% diluted bitumen (no silica particles), and (C) bitumen-treated silica particles in 4.5 wt% diluted bitumen. The collecting tray was located at depth of 3 cm.

Through differential settling, the asphaltene networks will grow in size and capture more silica particles as they travel downward. This increases the effective density of the asphaltene-silica complexes, and they will settle faster as a result (faster in comparison to asphaltene networks that are devoid of silica particles). This effect should become more apparent at greater depths. Figure 4.6 shows the settling curves for Cases A, B and C — with all conditions the same as before except for the depth of the collecting tray, which was lowered to 3.0 cm from the liquid surface. Similar to Figure 4.5, we note the important mass balance between Curve C and the sum of the steady state masses of Curves A and B. Moreover,

Curve C, which reflects the settling of the asphaltene-silica complexes, clearly shows a shorter sedimentation time compared to the case with only asphaltene networks (Curve B). It appears that the mechanism of differential settling, as a means of collecting the silica particles, becomes more important at greater depths.

4.2 Hetero-Aggregation of Solids

In contrast to homo-aggregation of solids, this part of the study is focused on the capture of fine particulates in the oil phase through interfacial attachment. In particular, a small amount of water is introduced into the hydrocarbon phase to create a network of oil-water interfaces which function as "particle traps." To gain insight into this process, particle-water droplet interactions are examined in solvent diluted bitumen using the micro-cantilever technique. The attachment forces are examined under a variety of relevant conditions, such as the addition of surfactants to the water phase and the dilution of the oil phase with solvent consisting of different volume ratios of *n*-heptane to toluene.

4.2.1 Adhesive Force Measurements

As in the previous study, the micro-cantilever technique was used to measure adhesive forces between water and solid in a hydrocarbon medium. To begin our study at a preliminary level, the measurements were conducted with DI water and untreated solid (i.e. glass), while the surrounding media was pure heptol (see Figure 3.3). As untreated (i.e. clean) glass is hydrophilic, the results provided the *maximum* possible force between the water droplet and the solid. As presented in

Figure 4.7, the adhesive force became stronger as the *n*-heptane content increased (and the toluene content decreased) in the heptol mixture. To rationalize these results, the interfacial tensions between water and heptol had been measured (presented in Table 4.1). Next, the corresponding capillary force F_{cap} was calculated based on the maximum wetted perimeter of the experimental pipette tip (radius of 10-15 μm) and the measured IFTs, i.e.

$$F_{\text{cap}} = (\text{IFT from Table 4.1}) \times 2\pi\,(\text{max. radius of pipette tip}) \qquad \text{Equation 4.2}$$

As expected, the calculated forces F_{cap} are within 10% of the micro-cantilever measurements (blue symbols in Figure 4.7).

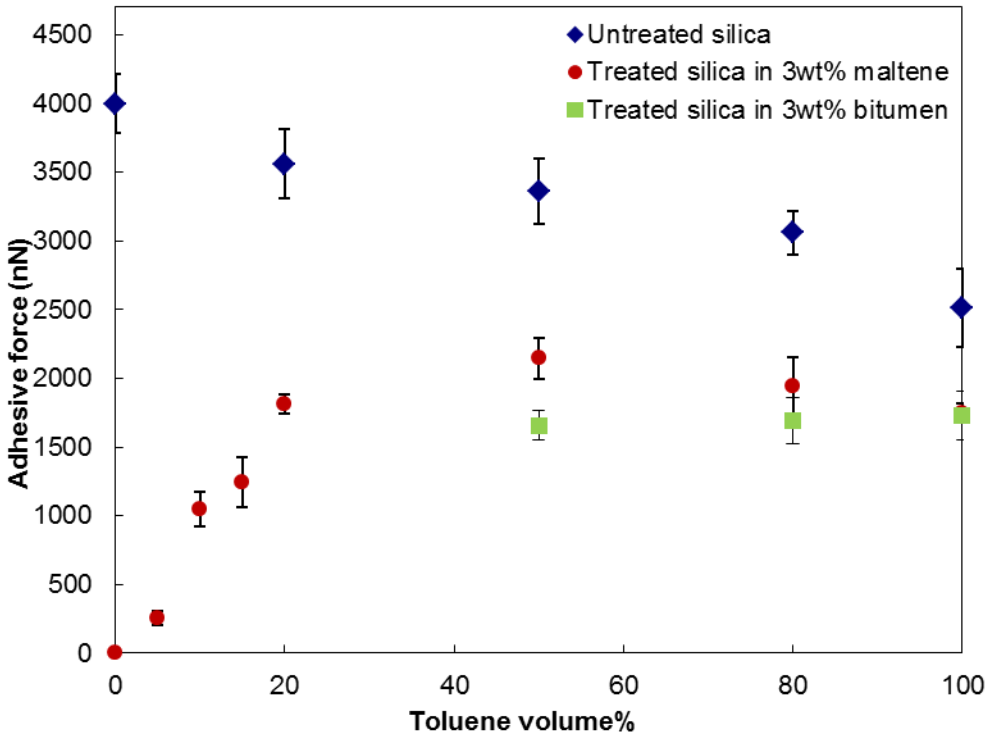

Figure 4.7. Measured adhesive forces for (a) clean (i.e. untreated) glass particles in heptol (◆); (b) effect of the addition of 3 wt% maltene (●), and (c) 3wt%

bitumen (■) on the adhesion force between bitumen-treated glass spheres and DI water in heptol.

Next, the above "basis system" was altered in two ways: (a) the solid glass tip was now surface-modified with bitumen, and (b) the heptol solution now had 3 wt% maltene. Adhesive forces between bitumen-treated glass tips and DI water "drops" were measured in the same way (Figure 3.3); the results are presented also in Figure 4.7 (red symbols). Let us begin examining the data points from the right, i.e. beginning from pure toluene: from 100 vol% to 50 vol% toluene, the measured forces (red symbols) were noticeably lower in comparison to those of the pure solvent system (blue symbols). This is not surprising as surface active components in maltene would lower the heptol-water interfacial tension, thus leading to weaker wetting forces between the solid and water [28, 55]. Indeed, the red symbols appeared to follow the same upward trend as the toluene concentration was lowered from 100 vol% to 50 vol%. However, this trend took a downward turn as the *n*-heptane content increased (i.e. the toluene content decreased); even more surprising was the fact that no adhesive force was detectable at 0 vol% toluene (i.e. in pure *n*-heptane). The same force measurement experiments were also conducted in the presence of 3 wt% full bitumen (i.e. maltene + asphaltene); the results are illustrated as the green symbols in Figure 4.7. As the data is viewed from right to left (i.e. beginning with 100% toluene), the measured forces appear to follow the same trend as in the case for diluted maltene. Unfortunately, as the toluene concentration fell below 50 vol%, the experiment could no longer proceed as the oil phase was filled with

asphaltene precipitates; these suspended entities severely obstructed the field of view and the ability to carry out micromechanical manipulations.

Table 4.1. Interfacial tensions between water and heptol at room temperature.

	Interfacial Tension (mN/m)	
Solvent	Present work	From ref. [29]
n-heptane	49.5 ± 0.5	50.9
20% vol toluene	43.3 ± 0.3	45
50% vol toluene	39.4 ± 0.05	39.6
80% vol toluene	37.6 ± 0.04	37.5
toluene	35.5 ± 0.04	36.1

The anomalous downward turn exhibited by the red symbols in Figure 4.7 (for toluene concentrations < 50 vol%) can be understood as follows: Figure 4.8 presents microscope images of our force measuring experiments in the presence of maltene. In toluene-diluted maltene (Figure 4.8(a)), the treated glass tip was wetted by the water and strong adhesion was observed. However, in heptane-diluted maltene, there was no wetting by the oil-water interface, and thus no attachment force was detected (Figure 4.8(b)). A higher magnification of the microscope image in *n*-heptane reveals formation of colloidal asphaltene precipitates. As seen in Figure 4.8(c), even though the experiment was conducted in diluted maltene, small residuals of asphaltene in the system were unavoidable. (Recall that asphaltene is defined as a solubility fraction and does not have a well-defined molecular structure; it is thus impossible to eliminate all such "molecules" in a maltene sample.) When the maltene is diluted in heptane, these

residual asphaltenes would form microscopic precipitates which evidently prefer to reside at the oil-water interface [56-58]. We speculate that the adsorption of asphaltene precipitates at the oil-water interface would lead to formation of a "protective skin" that stabilizes the water droplet: It prevents the wetting of the glass pipette tip (or equivalently, its penetration into the water drop) and results in zero attachment force between the water droplet and the solid (Figure 4.8(b)). As the toluene content in the solvent increases, this protective skin would disappear — presumably due to dissolution of the asphaltene precipitates by the aromatic solvent.

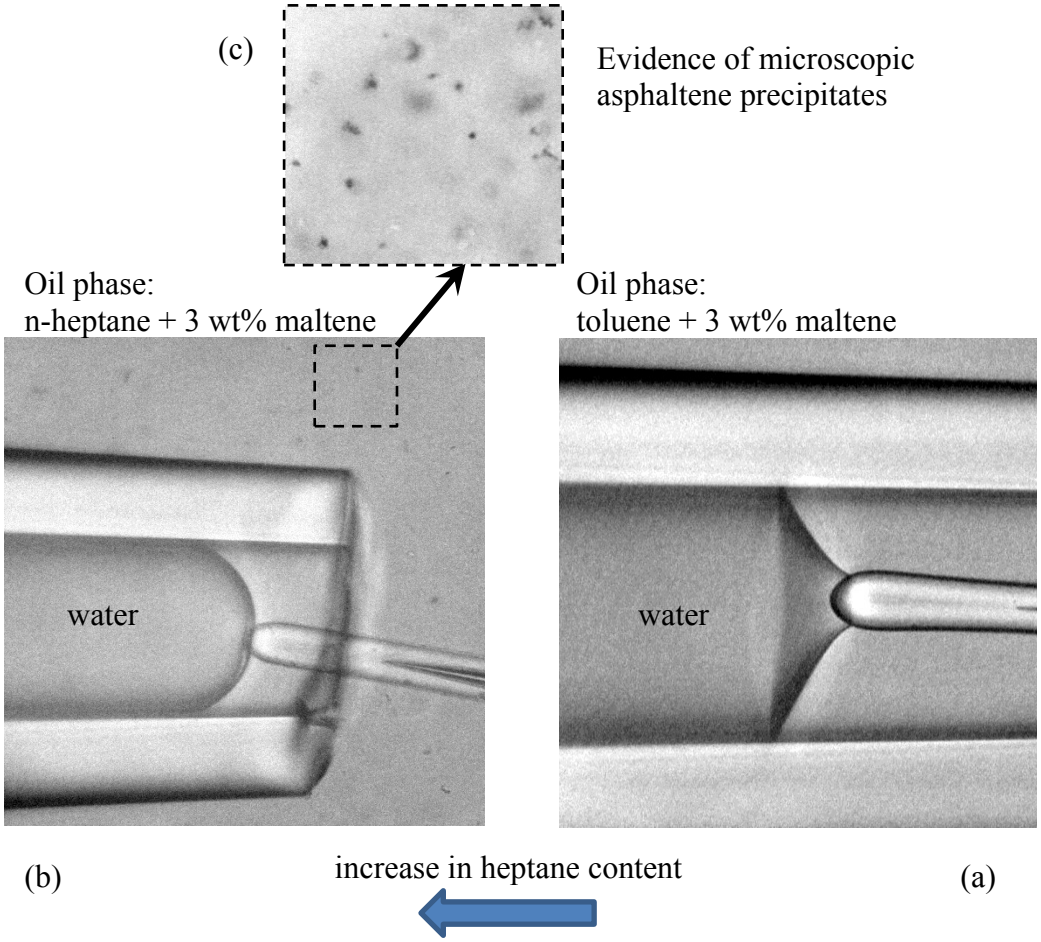

Figure 4.8. Microscope images of bitumen-treated pipette tip contacting water in hydrocarbon containing 3wt% maltene. The maltene was diluted in (a) toluene, (b) *n*-heptane. A magnified view of the heptane-diluted maltene solution is shown in (c); evidence of colloidal asphaltene precipitates can be seen in this magnified view.

The following tests were conducted to demonstrate the existence of the "protective skin": A micropipette filled with DI water was immersed into a solution of 3 wt% heptane-diluted maltene. Water was expelled slowly out of the pipette and formed a spherical droplet at the tip (the water in the droplet was still connected to that inside the pipette; see Figure 4.9 (a)). The water droplet was then allowed to age for 2 minutes, and a bitumen-treated pipette tip was used to

contact the oil-water interface. As the pipette was slowly pushed toward the center of the droplet, the skin did not rupture and showed resistance (Figure 4.9(b)). Following this, the water droplet was slowly deflated by withdrawing water back into the pipette. As the oil-water interface was compressed, a rigid adsorbed layer was visible in the form of a crumpled surface (Figure 4.9(c)). This observation is strong evidence of the formation of a protective skin in high *n*-heptane content.

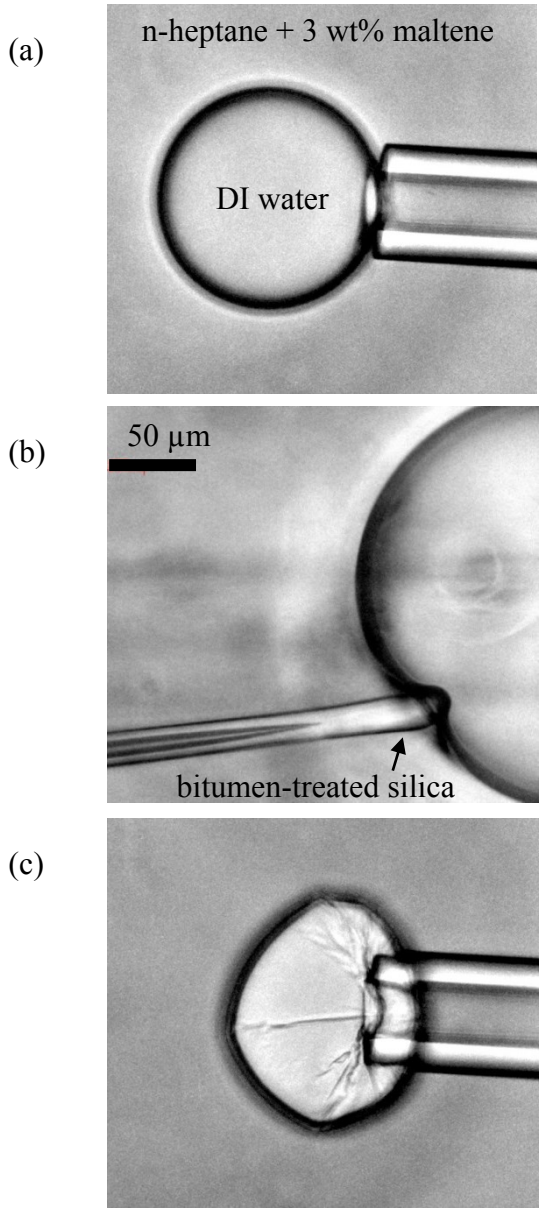

Figure 4.9. Evidence of a "protective skin" at the surface of a water droplet; the surrounding phase was 3 wt% heptane-diluted maltene. (a) A water droplet was formed at the tip of the pipette; (b) an attempt to use a bitumen-treated pipette tip to penetrate the water droplet; (c) as the water droplet was deflated, the protective skin was revealed in the form of a crumpled surface.

The above study suggests that the presence of a protective skin on the oil-water interface (for solvents of higher paraffinic content) interferes with the mechanism of solids capture. In all of the above scenarios, the aqueous phase was DI water. Here, we postulate that it is possible to customize the chemistry and composition of the aqueous phase to facilitate particle capture. For example, the addition of surfactants to the aqueous phase would decrease the oil-water interfacial tension, which is detrimental to the capture of unwanted solids; however, it may also disrupt the formation of a rigid skin and thus improve wettability (and hence the removal) of solids. To investigate these effects, we have conducted qualitative tests by adding different types of surfactants to the aqueous phase to examine their influence on the rigid skin.

The following experiments were conducted in heptane-diluted maltene (at 3 wt%) where no wetting — and thus zero attachment force — was observed between the treated solid and the oil-water interface (see Figure 4.8(b) and 4.9(b)). As mentioned in Sections 2.6 and 3.4.2, the four types of water-soluble surfactants chosen for this study are: CTAB (cetrimonium bromide), SDS (sodium dodecylsulfate), SDBS (sodium dodecylbenzenesulfonate) and SN (sodium naphthenates). All surfactant solutions were prepared above the critical micelle concentration (CMC) of the surfactant; the pH of the aqueous phase was measured at each stage. The critical micelle concentrations of CTAB, SDS, SDBS are well-known from literature [59]. The IFT isotherm of SN was measured in an earlier study in our group and the CMC was reported as 10 g/L

[46]. We have also conducted IFT measurements using the micropipette technique (discussed in Section 3.8) to map the IFT isotherms of SN in *n*-heptane and 3 wt% heptane-diluted maltene; the results are shown in Figure 4.10.

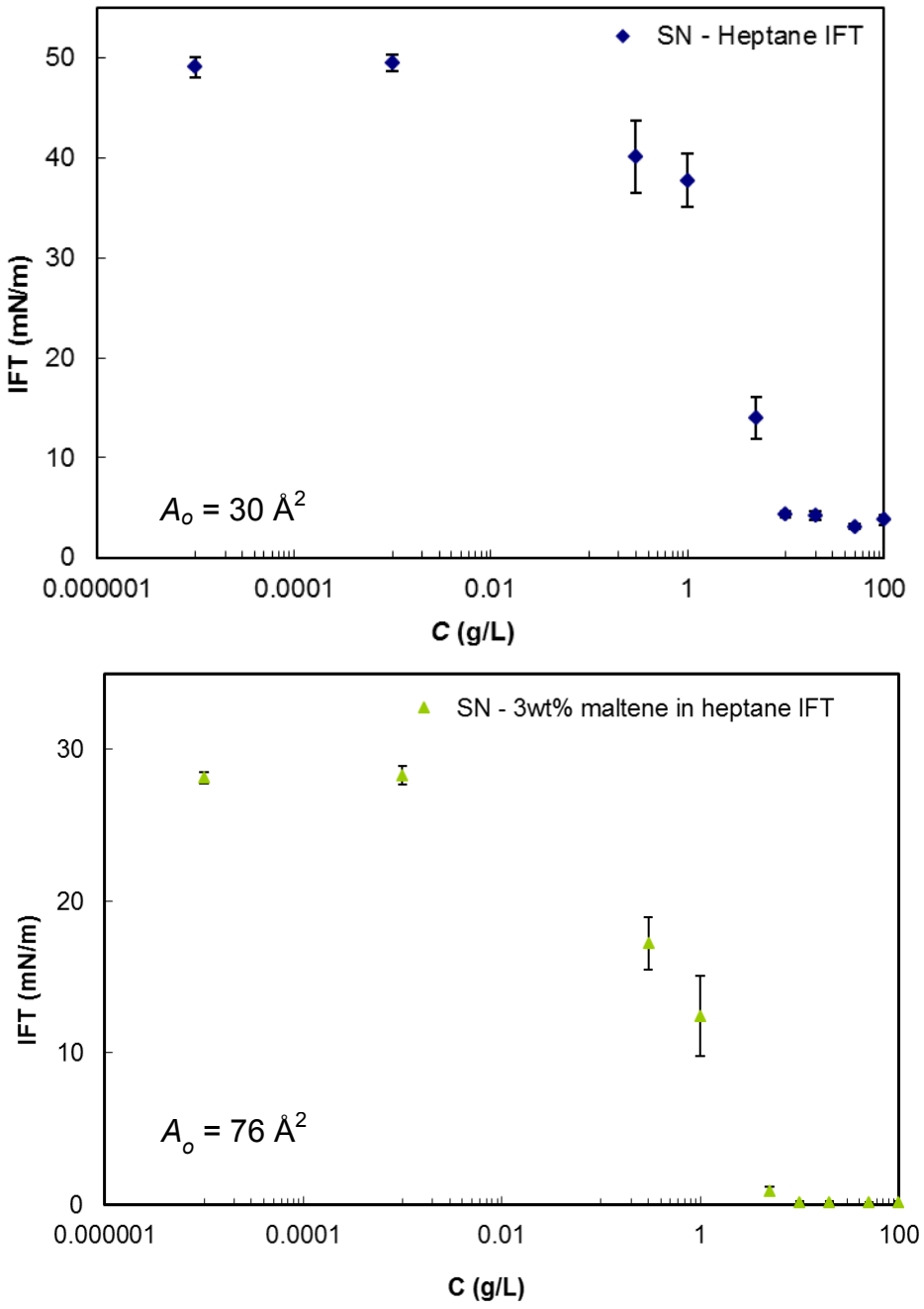

Figure 4.10. Interfacial tension (IFT) as a function of the sodium naphthenates concentration (C) in the aqueous phase; the oil phases were *n*-heptane (◆) and 3 wt% heptane-diluted maltene (▲).

In the following qualitative experiments, the aqueous droplet (containing water-soluble surfactants) was poked by a bitumen-treated pipette tip to check for the existence of the protective skin. With addition of CTAB (pH 4 and 8) to the water phase, no attachment was observed between the solid and aqueous phase; this indicated the presence of the protective skin. With addition of SDS (pH 8) and SDBS (pH 8), the rigid skin showed an initial resistance to the poking; however, weak attachment between the water droplet and the solid tip was observed. In contrast, addition of SN (pH 10) completely prevented the formation of the protective skin and, as a result, strong attachment was observed at the oil-water interface. As mentioned earlier (Section 2.6), SN is indigenous to bitumen and has favorable interfacial properties (i.e. ability to lower interfacial tension) [46, 48]. Therefore, it is an ideal candidate as an additive in fine solids removal (i.e. using emulsified water droplets are 'solids collectors,' with the surfactants present inside the droplets).

We now focus on SN as the surfactant of choice. Using the micro-cantilever technique, attachment forces between the aqueous phase and the treated solid were measured. The aqueous solution contained SN at different concentrations (ranging from 0 to 10 g/L, the upper limit being the CMC), and the oil phase consisting of 3wt% maltene in *n*-heptane. The results of the force measurement are shown in Figure 4.11 (blue symbols). These forces suggest that there is an

optimal surfactant concentration; the trade-off is due to the fact that SN addition has the desirable function of disrupting the rigid skin formation, but also the detrimental effect of lowering the IFT, and thus weakening the attachment force. As seen, addition of a small amount of SN (0.3 g/L) was enough to disrupt the formation of the protective skin. Indeed, we believe that there is a competition between SN and the asphaltene molecules for the oil-water interface.

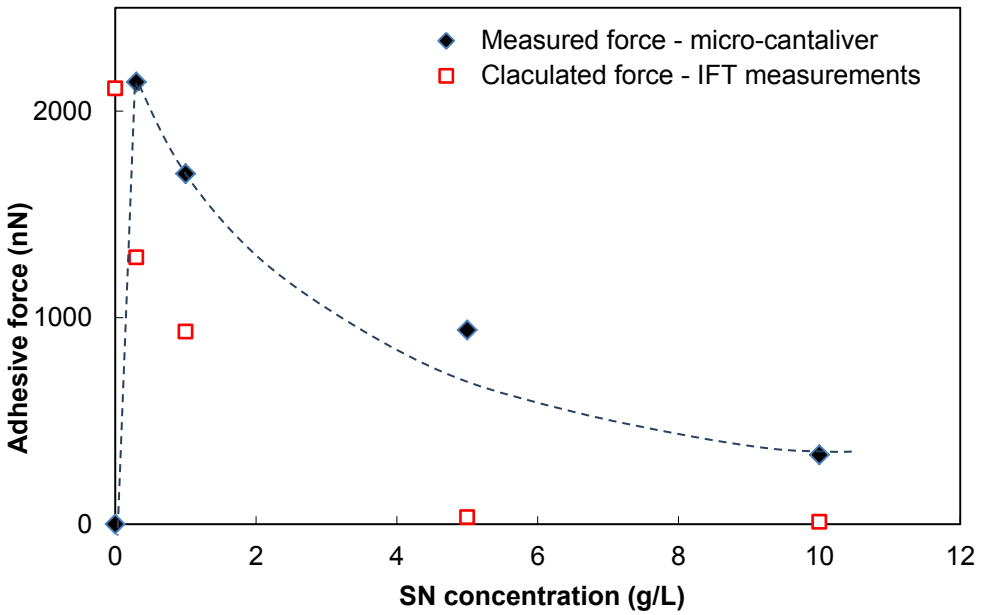

Figure 4.11. Using the micro-cantilever technique, attachment forces between water droplets containing SN and bitumen-treated solids, both immersed in 3wt% heptane-diluted maltene, were measured (◆). The calculated capillary forces (□) were based on the measured IFTs presented in Figure 4.10.

As a consistency check, capillary forces on the treated solids (with radii of 10-15 μm) were also calculated based on the measured IFTs in Figure 4.10. The results of these calculations are presented in Figure 4.11 (the red symbols).

It is interesting that the calculated forces are significantly lower than those measured by the micro-cantilever experiment. This difference may be explained by the rheological properties of the oil-water interface which resulted from formation of the protective skin. The rheology of such interfaces can be a strong function of the extent and rate at which the surface is deformed. Deformation of the oil-water interface is more and faster in the micro-cantilever force measurement experiment; hence, the directly-measured forces are larger than those calculated based on the IFTs.

It is also worth noting that the maximum calculated force is reported at zero SN concentration (i.e. DI water); this is another consequence of neglecting the existence of the rigid layer when calculating the capillary force.

5. Conclusions

5.1 General summary

One major challenge in the solvent-based extraction of bitumen (from mined Athabasca oil sands) is the removal of fine solids from non-aqueous liquids. Removal of fine solids by the usual means of separation, such as filtration or centrifugation, is not practical. To accomplish fine solids removal, it is imperative to first understand the colloidal interactions that are relevant to the process. Two possible scenarios have been put forward for the removal of bitumen-adsorbed solids from organic liquids: (a) through homo-aggregation of the solids (i.e. aggregation of the particles amongst themselves), and (b) using emulsified water as collector — to capture the solid particles at the oil-water interfaces.

In the first part of this study, the physics behind the homo-aggregation of solids was studied on the macro- and micro-scales using, respectively, sedimentation tests and the novel micro-cantilever technique. It was observed that in a paraffinic environment, the colloidal interactions between solids result in homo-aggregation and sedimentation of the solids. However, as the aromatic content of the solvent was increased, very weak or zero inter-particle forces were detected. To rationalize these observations, we propose that when the solid surfaces are modified by bitumen (i.e. exposed to bituminous material for extended periods of time), the surface-adsorbed molecules will display extended conformations in an

aromatic environment, forming a "swollen brush" — and a steric barrier — around the particle. If the aromatic solvent were replaced with one that is paraffinic, the molecular brush will collapse onto the surface, giving rise to negligible steric repulsion between the particles. In short, we are suggesting that the adsorbed molecules are "asphaltene-like" (see Figure 4.4). Going further with this molecular picture, we speculate that the thickness of the adsorbed layer will depend on the aromatic content of the solvent; this will in turn influence strongly the magnitude of the inter-particle forces.

In non-aqueous liquids, the two main colloidal forces between bitumen-treated surfaces are van der Waals attraction and steric repulsion; the interplay of these two interactions in pure heptol (i.e. heptane + toluene) was clearly demonstrated through the adhesive forces in Figure 4.3 (the blue symbols). Addition of maltene to heptol will change both the refractive index of the solvent and the separation distance between the particles; these will cause an overall decrease in inter-particle interactions (Figure 4.3) and, consequently, the settling rates (Figure 4.2).

Addition of full bitumen (can be viewed here as maltene + asphaltene) to the heptol solvent, however, results in formation of asphaltene precipitates at higher heptane contents. These precipitates suppress the homo-aggregation of the solid particles, mostly likely through physical intervention (i.e. intervening between the solid particles and preventing their close approach). However, even with the absence of solids homo-aggregation, all the particles were captured by the asphaltene networks and asphaltene-silica complexes (Section 4.1.3).

In the next part of this study, we examined the use of water droplets as collectors of solid particles in organic solvents (i.e. the solid-water hetero-aggregation). Particle-water interactions were examined in heptol-diluted maltene using the micro-cantilever technique. As bitumen naturally contains surface active materials, addition of maltene to heptol decreased the heptol-water interfacial tension. As a result, the solid-water attachment forces in such systems were weaker compared to those in pure heptol. Surprisingly, when there was very little or no aromatic content in heptol, no adhesion was observed between the treated particle and the oil-water interface (see Figure 4.7). This phenomenon was attributed to the formation of a "rigid skin" at the diluted maltene-water interface at higher heptane contents. In particular, it was observed that precipitates of residual asphlaltene in the "pure maltene solution" accumulated and formed a rigid layer at the oil-water interface; the presence of this rigid skin limited, or prevented entirely, wetting of the solid by the water drop (Figures 4.8(b) and 4.9). For this segment of the investigation, we noted that the notion a "pure maltene" sample is unfounded, as "maltenes" and "asphaltenes" are differentiated as solubility fractions; their distinction is not molecularly based.

We have suggested the use of sodium naphthenates (SN), a natural surfactant indigenous to bitumen, as an additive to the water phase to interfere with rigid skin formation. We observed that SN successfully "won" the competition against asphaltene molecules for occupation of the oil-water interface, thus preventing formation of the rigid skin. However, the significant surface activity of SN also

lowered the oil-water interfacial tension and in turn weakened the solid-water attachment forces to perhaps unacceptable levels.

In summary, two mechanisms of capturing fine solids in organic liquids (heptol + bitumen) were introduced in this study: (a) homo-aggregation, and (b) hetero-aggregation. The "effectiveness" of each mechanism (a still-qualitative descriptor at this point) as a function of the toluene content in the heptol solvent is summarized in Figure 5.1.

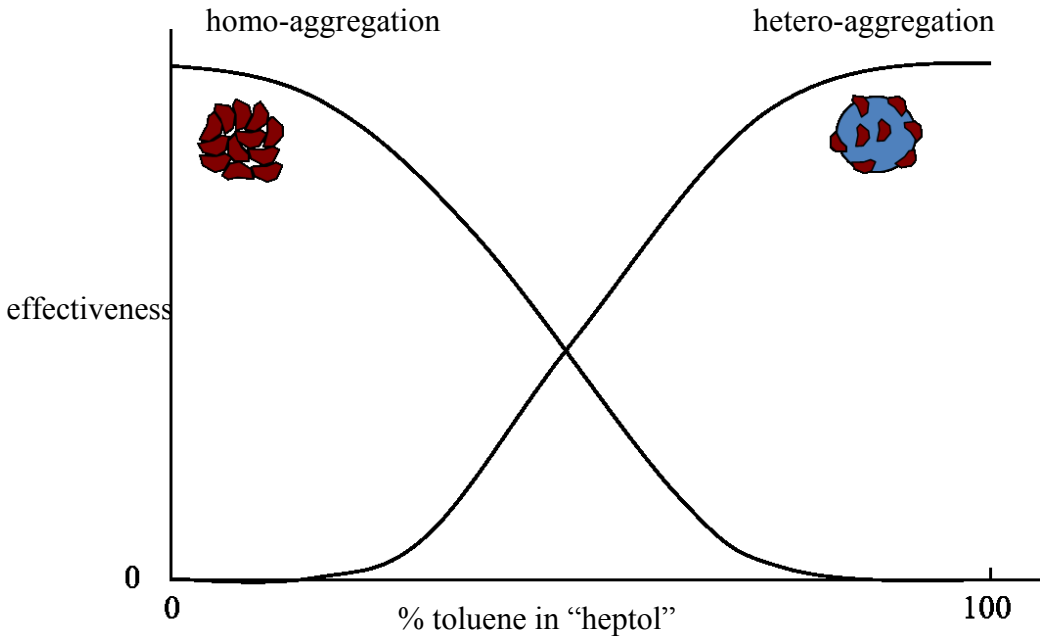

Figure 5.1. Comparing the aggregative effectiveness of the two mechanisms of solids capture (homo-aggregation and hetero-aggregation) in heptol. Note that "effectiveness" is only a qualitative descriptor in this presentation.

5.2 Recommendations and Challenges

For future work, it would be of great interest to change the type of organic solvent, and also the degree of bitumen and maltene dilution in both settling and force measurement tests. In this study, increase in dilution beyond 5 wt% of bitumen was challenging due to strong reduction in visibility. A possible solution can be decreasing the oil solution thickness under the microscope through changing the glass chamber containing the oil phase (Section 2.4.4).

One of the future focuses should be on increasing the solids concentration in the settling tests, and also the use of irregularly shaped particles (such as crushed minerals or clays) in both settling and force measurement tests. Findings from such studies will be much more realistic.

Also, it would be interesting to explore the addition of emulsified water to the settling tests. Parameters which will be of importance are: pH, salinity and addition of surfactants.

Finally, it would be interesting to develop a mathematical model to understand the kinetics of aggregation and sedimentation of the particles. Connecting model predictions to experimental test results can provide a deeper understanding of the aggregating behaviors of the particles.

References

[1] Woynillowicz D, Severson-Baker C, Raynolds M. Oil sands fever: The environmental implications of canada's oil sands rush. The Pembina Institute 2005.

[2] Board NE. Canada's oil sands - opportunities and challenges to 2015: An update. An Energy Market Assessment 2006.

[3] Sparks BD, Meadus FW. A combined solvent extraction and agglomeration technique for the recovery of bitumen from tar sands. Energy Processing Canada 1979;55-61.

[4] Sparks BD, Meadus FW. Study of some factors affecting solvent losses in the solvent extraction - spherical agglomeration of oil sands. Fuel Processing Technology 1981;4(4):251-64.

[5] Meadus FW, Chevrier PJ, Sparks BD. Solvent extraction of athabasca oil-sand in a rotating mill-1. Dissolution of bitumen Fuel Processing Technology 1982;6(3):277-87.

[6] Meadus FW, Bassaw BP, Sparks BD. Solvent extraction of athabasca oil-sand in a rotating mill-2. Solids-liquid separation and bitumen quality Fuel Processing Technology 1982;6(3):289-300.

[7] Sparks BD, Meadus FW, Hoefele EO. Solvent extraction spherical agglomeration of oil sands US Patent 1988.

[8] Xu Y, Dabros T, Hamza H. Study on the mechanism of foaming from bitumen froth treatment tailings. Journal of Dispersion Science and Technology 2007;28(3):413-8.

[9] Long Y, Dabros T, Hamza H. Stability and settling characteristics of solvent-diluted bitumen emulsions. Fuel 2002;81(15):1945-52.

[10] Romanova UG, Yarranton HW, Schramm LL, Shelfantook WE. Investigation of oil sands froth treatment. Canadian Journal of Chemical Engineering 2004;82(4):710-21.

[11] Yang X, Czarnecki J. The effect of naphtha to bitumen ratio on properties of water in diluted bitumen emulsions. Colloids and Surfaces A: Physicochemical and Engineering Aspects 2002;211(2-3):213-22.

[12] Romanova UG, Valinasab M, Stasiuk EN, Yarranton HW, Schramm LL, Shelfantook WE. The effect of oil sands bitumen extraction conditions on froth treatment performance. Journal of Canadian Petroleum Technology 2006;45(9):36-45.

[13] Chia J, Yeung A. Strength of asphaltene clusters in heptane-diluted bitumen. Fuel 2004;83(4-5):619-21.

[14] Madge DN, Garner WN. Theory of asphaltene precipitation in a hydrocarbon cyclone. Minerals Engineering 2007;20(4):387-94.

[15] Jin Y, Liu W, Liu Q, Yeung A. Aggregation of silica particles in non-aqueous media. Fuel 2011;90(8):2592-7.

[16] Oliver DR. The sedimentation of suspensions of closely-sized spherical particles. Chemical Engineering Science 1961;15(3-4):230-42.

[17] Eckert WF, Masliyah JH, Gray MR, Fedorak PM. Prediction of sedimentation and consolidation of fine tails. AIChE Journal 1996;42(4):960-72.

[18] Rhodes MJ. Introduction to particle technology. 2 ed.: Wiley; 2008.

[19] Zahabi A, Gray MR, Czarnecki J, Dabros T. Flocculation of silica particles from a model oil solution: Effect of adsorbed asphaltenes. 2010;243616-23.

[20] Butt H-J, Graf K, Kappl M. Physics and chemistry of interfaces. Wiley-VCH; 2003.

[21] Israelachvili J, Adams G. Measurement of forces between two mica surfaces in aqueous electrolyte solutions in the range 0–100 nm. Journal of the Chemical Society, Faraday Transactions 1 1978;74975 - 1001.

[22] Binnig G, Quate CF, Gerber C. Atomic force microscope. Physical Review Letters 1986;56(9):930-3.

[23] Prieve DC. Measurement of colloidal forces with tirm. Advances in Colloid and Interface Science 1999;82(1-3):93-125.

[24] Evans E, Needham D. Physical properties of surfactant bilayer membranes: Thermal transitions, elasticity, rigidity, cohesion and colloidal interactions Journal of Physical Chemistry 1987;91(16):4219-28.

[25] Evans EA, Skalak R, Hochmuth RM. Mechanics and thermodynamics of biomembranes 1. Crc Critical Reviews in Bioengineering 1979;3(3):181-330.

[26] Yeung AKC, Pelton R. Micromechanics: A new approach to studying the strength and breakup of flocs. Journal of Colloid and Interface Science 1996;184(2):579.

[27] Yeung A, Dabros T, Masliyah J. Does equilibrium interfacial tension depend on method of measurement? Journal of Colloid and Interface Science 1998;208(1):241-7.

[28] Moran K, Czarnecki J. Competitive adsorption of sodium naphthenates and naturally occurring species at water-in-crude oil emulsion droplet surfaces. Colloids and Surfaces A: Physicochemical and Engineering Aspects 2007;292(2-3):87-98.

[29] Moran K, Yeung A, Masliyah J. Factors affecting the aeration of small bitumen droplets. Canadian Journal of Chemical Engineering 2000;78(4):625-34.

[30] Moran K, Yeung A, Masliyah J. Shape relaxation of an elongated viscous drop. Journal of Colloid and Interface Science 2003;267(2):483-93.

[31] Moran K, Yeung A, Masliyah J. Measuring interfacial tensions of micrometer-sized droplets: A novel micromechanical technique. Langmuir 1999;15(24):8497-504.

[32] Hartley PG, Grieser F, Mulvaney P, Stevens GW. Surface forces and deformation at the oil-water interface probed using afm force measurement. Langmuir 1999;15(21):7282-9.

[33] Liu J, Zhang L, Xu Z, Masliyah J. Colloidal interactions between asphaltene surfaces in aqueous solutions. Langmuir 2006;22(4):1485-92.

[34] Liu J, Xu Z, Masliyah J. Studies on bitumen−silica interaction in aqueous solutions by atomic force microscopy. Langmuir 2003;19(9):3911-20.

[35] Liu J, Xu Z, Masliyah J. Role of fine clays in bitumen extraction from oil sands. AIChE Journal 2004;50(8):1917-27.

[36] Snyder BA, Aston DE, Berg JC. Particle−drop interactions examined with an atomic force microscope. Langmuir 1997;13(3):590-3.

[37] Johnson HE, Hu HW, Granick S. Mass adsorbed and surface forces in ternary solution as nonsolvent was added to the point of precipitation: Polystyrene in mixtures of cyclopentane and linear pentane. Macromolecules 2002;24(8):1859-67.

[38] Marra J, Hair ML. Interactions between adsorbed polystyrene layers in toluene-heptane mixtures. Effect of solvent quality. Macromolecules 2002;21(8):2349-55.

[39] Bergström L, Blomberg E. Probing polymeric stabilization in nonaqueous media by direct measurements. Journal of the American Ceramic Society 2000;83(1):217-19.

[40] Briscoe WH, Horn RG. Direct measurement of surface forces due to charging of solids immersed in a nonpolar liquid. Langmuir 2002;18(10):3945-56.

[41] Wang S, Liu J, Zhang L, Xu Z, Masliyah J. Colloidal interactions between asphaltene surfaces in toluene. Energy and Fuels 2009;23(2):862-9.

[42] Wang S, Liu J, Zhang L, Masliyah J, Xu Z. Interaction forces between asphaltene surfaces in organic solvents. Langmuir 2010;26(1):183-90.

[43] Natarajan A, Xie J, Wang S, Masliyah J, Zeng H, Xu Z. Understanding molecular interactions of asphaltenes in organic solvents using a surface force apparatus. Journal of Physical Chemistry C 2011;115(32):16043-51.

[44] Zahabi A, Gray MR, Dabros T. Heterogeneity of asphaltene deposits on gold surfaces in organic phase using atomic force microscopy. 2012;262891-8.

[45] Masliyah JH, Xu Z, Czarnecki JA. Handbook on theory and practice of bitumen recovery from athabasca oil sands. Kingsley Publishing Services; 2011.

[46] Afshar S, Mirmontazeri L, Yeung A. Potential use of naphthenic acids in soil remediation: Examination of pore-scale interfacial properties. Fuel 2014;116:395-8.

[47] Horvath-Szabo G, Masliyah JH, Czarnecki J. Phase behavior of sodium naphthenates, toluene, and water. Journal of Colloid and Interface Science 2001;242(1):247-54.

[48] Cyr TD, Strausz OP. Bound carboxylic acids in the alberta oil sands. Organic Geochemistry 1984;7(2):127-40.

[49] Yang X, Czarnecki J. Tracing sodium naphthenate in asphaltenes precipitated from athabasca bitumen. Energy & Fuels 2005;19(6):2455-9.

[50] Gu G, Xu Z, Nandakumar K, Masliyah JH. Influence of water-soluble and water-insoluble natural surface active components on the stability of water-in-toluene-diluted bitumen emulsion. Fuel 2002;81(14):1859-69.

[51] Yeung A, Dabros T, Czarnecki J, Masliyah J. On the interfacial properties of micrometer-sized water droplets in crude oil The Royal Society 1999;4553709-23.

[52] Yeung A, Dabros T, Masliyah J, Czarnecki J. Micropipette: A new technique in emulsion research. Colloids and Surfaces A: Physicochemical and Engineering Aspects 2000;174(1-2):169-81.

[53] Fotland P, Askvik KM. Determination of hamaker constants for asphaltenes in a mixture of pentane and benzene. Colloids and Surfaces A: Physicochemical and Engineering Aspects 2008;324(1-3):22-7.

[54] Taylor SD, Czarnecki J, Masliyah J. Refractive index measurements of diluted bitumen solutions. Fuel 2001;80(14):2013-8.

[55] Gao S, Moran K, Xu Z, Masliyah J. Role of bitumen components in stabilizing water-in-diluted oil emulsions. Energy & Fuels 2009;23(5):2606-12.

[56] Yarranton HW, Alboudwarej H, Jakher R. Investigation of asphaltene association with vapor pressure osmometry and interfacial tension measurements. Industrial and Engineering Chemistry Research 2000;39(8):2916-24.

[57] Mohamed RS, Ramos AnCS, Loh W. Aggregation behavior of two asphaltenic fractions in aromatic solvents. Energy & Fuels 1999;13(2):323-7.

[58] Yarranton HW, Hussein H, Masliyah JH. Water-in-hydrocarbon emulsions stabilized by asphaltenes at low concentrations. Journal of Colloid and Interface Science 2000;228(1):52-63.

[59] Mukerjee P. Critical micelle concentrations of aqueous surfactant systems. U.S. National Bureau of Standards; 1932.

Appendix A - Calculating the Micro-Cantilever Stiffness

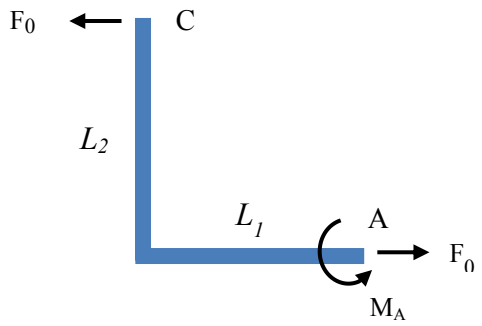

Figure A. 1. Free body diagram of the micro-cantilever [31].

A free body diagram of the cantilever is shown in Figure A.1. A known quantity of axial load F_0 is applied at point C (i.e. the tip of the cantilever). The L-shaped structure is fixed at point A; at this point the cross section diameter is large enough to be consider immovable. The length L_2 is typically 5-6 mm and the length L_1 should be more than 100 μm. To have zero body rotation the bending moment at A can be defined by the following equation [31]:

$$M_1(x_1) = -F_0 L_2 \tag{A1}$$

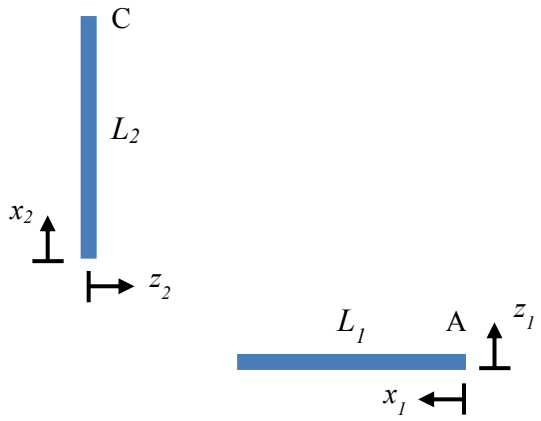

Figure A. 2. Deviding the cantaliver into two straight members, with coordinates as defined. The moment-curvature relation for slender beams (eq A2) can be applied to each individual member of evaluation of deflections [31].

To analyze the moment on the cantilever, the L-shaped structure has been broken into two straight sections L_1 and L_2 (Figure A.2). z_1 and z_2 (i.e. tranverse deflections of L_1 and L_2 straight sections) can be assumed to be negligible compared to their beam length. Hence, the slender beams moment-curvature equation can be applied:

$$\frac{d^2 z_i}{dx_i^2} = \frac{M_i}{EI_i} \qquad i = 1,2 \tag{A2}$$

Integrating equation A2 the bending moment in the two sections are:

$$M_1(x_1) = -F_0 L_2$$

$$M_2(x_2) = -F_0 L_2 \left(1 - \frac{x_2}{L_1}\right) \tag{A3}$$

where I is the moment of inertia of a hollow cylinder. This parameter can be calculated by:

$$I = \frac{\pi}{4} r_{out}^4 \left(1 - \left(\frac{r_{in}}{r_{out}}\right)^4\right) \quad \text{(A4)}$$

Please note that as a result of the cantilever tapering, the cross section of the cantilever has a variable diameter moving along the axial direction. It is observed that r_{in}/r_{out} for heat tapered capillary stays constant; in this study the value has been set as 0.6. The next step to calculate I is to measure r_{out} at various location throughout the cantilever (e.g. 10 points per straight section) and intermediate I values [31].

Appendix B - Evaluation of Naphthenic Acids as a Soil Remediation Agent: A Physicochemical Perspective

Leyli Mirmontazeri, Shima Afshar, and Anthony Yeung

Department of Chemical & Materials Engineering, University of Alberta,

Edmonton, Alberta, T6G 2V4, Canada.

Abstract

Removal of residual oil from reject sand grains is a major challenge in solvent-based bitumen extraction. A proposed solution is to wash the oil-contaminated sand grains with water and surfactants (the remediation agent). Due to the very favourable interfacial properties of naphthenic acids, namely, its ability to significantly reduce the oil-water interfacial tension and render the solid substrate hydrophilic, the surfactant has been proposed as a promising remediation agent. In this study, we evaluated the washing performance of naphthenic acids and demonstrated its inadequacy in sand remediation. The fundamental reason for the surfactant's poor performance was the inadvertent formation of a bicontinuous microemulsion which consumed much of the naphthenic acids, leaving little if any for remediation purposes.

1. Introduction

At present, the primary method of extracting bitumen (extra heavy oil) from the Canadian oil sands is a flotation process which produces, as a by-product, contaminated water which must be kept in increasingly large tailings ponds [1, 2]. To address this problem, recent efforts are under way to develop alternative solvent-based extraction methods which require little or no water [3, 4]. Briefly, a solvent-based process involves mixing mined oil sand with a light hydrocarbon solvent, creating (i) a product in the form of diluted bitumen, and (ii) a reject stream which consists of the left-over sand grains. Owing to capillary forces, there will unavoidably be residual diluted bitumen that is trapped within the small crevices between the sand particles. As this residual oil has in it a volatile organic component (the solvent), it must be separated from the sand before the latter can be used for land reclamation. Indeed, the primary obstacle to any solvent-based extraction technology is the removal of residual oil from the reject sand grains.

In separating the residual oil, straightforward methods such as mechanical displacement and drying are effective only up to a point (the last portion of the oil is most difficult to remove). An alternative approach, one that we recently began to explore, is to wash the oil-laden sand particles with water-surfactant systems. This is a technique that is often employed in soil remediation [5, 6], and shares many similarities with chemical enhanced oil recovery [7, 8]. As the intent of solvent-based extraction is to avoid excessive consumption of water, the washing process must be in accordance with the principle of minimal water use (using an

amount that is, for example, equal to that of the residual oil). With little water at one's disposal, the effectiveness of the surfactant becomes especially critical to the success of a washing operation. Unfortunately, no clear guideline can be found in the literature regarding the choice of surfactants for soil remediation: the 'optimal' surfactant appears to depend on the type of soil and the nature of the contamination; there is also no consensus on the chemical structure of the surfactant (e.g. whether it should be anionic or non-ionic) or the dosage that should be applied (e.g. whether it is above or below the critical micelle concentration) [9, 10]. With little guidance from field-based experience, we turn our focus to the fundamentals of colloid and interface science. There are several conditions that a good washing agent should satisfy: Recognising that the residual oil is held in place by capillary forces, the first requirement of a washing agent is its ability to significantly lower the oil-water interfacial tension γ. In addition, a small contact angle θ_c between the oil-water interface and the silica surface (angle measured through the aqueous phase) would greatly facilitate detachment of oil ganglia from the sand. Lastly, the surfactant should also be abundant and readily available to the operator. In an earlier paper, we had demonstrated that a particular class of surfactants, called naphthenic acids (NA), fulfils all of the above requirements [11]. Naphthenic acids is a class of anionic surfactants (consisting of cycloalkane carboxylic acids) that is indigenous to the Athabasca bitumen and many other types of crude oils [12-14]; it has an abundance of 1–2wt% in Athabasca bitumen [15]. Our earlier study showed that

NA had just the desired pore-scale interfacial properties for a washing process, i.e. it was able to create low γ and small θ_c [11]. Along with its ready availability, it appears naphthenic acids is an ideal candidate as a washing agent. In this study, we take the next logical step and evaluate the performance of naphthenic acids as an agent for cleaning oil-contaminated sand grains. We will demonstrate that, despite its promising interfacial properties, NA performs rather poorly as a washing agent. As such, we are reporting a negative finding. The main focus of this communication, however, is not on identification of a viable washing agent; rather, it is to reveal, from a fundamental perspective, the underlying mechanisms that led to NA's poor performance. The learning from this study, perhaps as a cautionary note, can be of relevance to many soil remediation and chemical enhanced oil recovery operations.

2. Experimental

Surface Treatment of the Sands

Before experiments, the sand grains were pre-treated under controlled conditions as follows: "Quack sand" (silica grinding sand with average diameter of 0.8 mm) was purchased from Quackenbush Company Inc. (Crystal Lake, Illinois) and used as the solid matrix. The sand was first thoroughly washed in toluene (HPLC grade) and dried under convective air flow. The particles are next surface-treated by dispersing them in 10 wt% diluted bitumen (i.e. 1 part bitumen + 9 parts toluene) to allow extensive exposure of the silica to bituminous materials — just

as in the case of the waste sand grains in a solvent-based extraction operation. Bitumen samples (the so-called "DRU bottoms") were obtained from Syncrude Canada Ltd. The sand particles were suspended and stirred in the diluted bitumen solution for two days, then washed multiple times with toluene until all residual diluted bitumen was rinsed away; the particles were again allowed to dry under a fume hood. This pre-treatment step was to render the sand particles hydrophobic: exposure to diluted bitumen would cause irreversible adsorption of bituminous materials onto the silica surface, despite subsequent washing of the particles in toluene [16, 17].

Surfactant Solution and Its Surface Tension

Naphthenic acids was the surfactant used in this study. Sodium naphthenates (SN), which is the salt form of naphthenic acids, was supplied by Eastman Kodak (practical grade) as a yellowish crystalline material. The Kodak SN was used without further purification. Aqueous solutions of sodium naphthenates were prepared at various concentrations by dissolving the SN crystals in deionised and distilled water. To speed up the dissolution process, the mixtures were placed in a sonication bath for 1 to 2 minutes. It is known from an earlier study that the critical micelle concentration (CMC) of SN is roughly 10 g/L [11]. The surface tensions of SN solutions were measured by a Krüss K100 device with a Wilhelmy plate.

Washing Protocol

We devised the following protocol to quantify the overall performance of a washing agent. Here, "overall performance" includes the ability of the surfactant to: liberate oil fragments from the sand grains, emulsify the oil in the aqueous phase, and facilitate transport of the oil/water mixture out of the porous sand matrix. In accordance with the principle of minimal water use (see Introduction), we also stipulated, somewhat arbitrarily, that the amount of water consumption would be equal to the amount of oil that was to be washed.

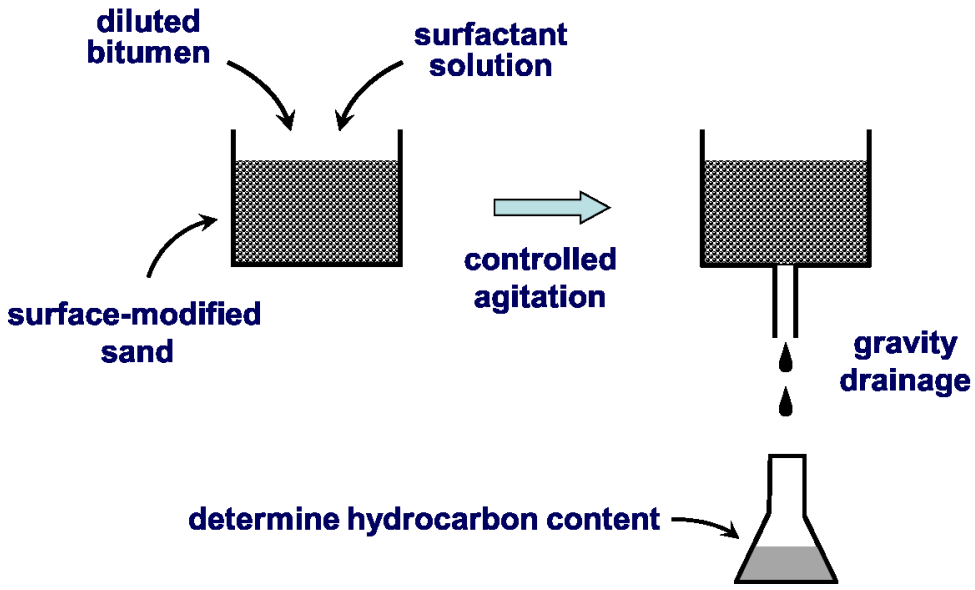

Figure 1. A schematic of the washing protocol. Surface-modified sand was first "contaminated" with diluted bitumen, then washed with an aqueous surfactant solution that is equal in mass to the contaminant. The amount of hydrocarbon in the drained liquid is used as a measure of the washing performance.

Figure 1 shows a schematic of the washing procedures. As a first step, 50.0 g of surface-treated sand was placed in a PTFE (i.e. Teflon®) bottle. The bottle was gently tapped on a hard surface until the dry sand grains were more-or-less

"close-packed" (i.e. with the sand level in the bottle at its lowest). Next, the sand was "contaminated" by slowly dripping toluene-diluted bitumen (again at 10 wt% concentration) into the PTFE bottle until the sand matrix was saturated with the liquid — and before the grains were completely submerged. The amount of diluted bitumen required for this step was very repeatable: it was 8.0 g. To remediate (i.e. clean) the oil-wetted sand, 8.0 g of an aqueous surfactant solution was introduced into the PTFE bottle containing the oil/sand mixture; the concentration of SN in the aqueous solution ranged from 0 to 100 g/L (recall that the CMC is ~10 g/L). Next, the oil/water/sand mixture was agitated in one of two ways: (a) Gentle mixing with a spatula for 2 min, at a period of about 5 s per revolution; (b) vigorous shaking on an Excella E2 platform shaker (New Brunswick Scientific) at 300 rpm for 2 min. We will refer to these two manners of mixing as the low and high shear agitations, respectively; the corresponding shear rates are estimated to be of order 1 s^{-1} and 100 s^{-1}. Following agitation, the mixture was transferred to a glass vacuum filter holder (filtration area 9.6 cm^2; Fisherbrand, Fisher Scientific) and the oil/water mixture was allowed to drain through a stainless steel screen (100 mesh) and into a collecting flask until the dripping stopped. (Note that this filtration/drainage step was carried out without any filter paper or vacuum suction.) The drained liquid is a mixture of diluted bitumen, water and surfactants in various emulsified and/or free forms. To calculate the washing efficiency, we needed to determine the amount of contaminant (i.e. diluted bitumen) contained in the drained mixture. To that end,

we found it easier to instead measure the bitumen content (at 10 wt% concentration, the mass of diluted bitumen is 10× that of the bitumen); this was done as follows: The drained liquid, which typically varied between 8 to 10 mL in volume, was mixed with 200 mL of water and 200 mL of dichloromethane. This new mixture of more than 400 mL was shaken vigorously for 2 min in a separatory funnel and left to equilibrate for 24 hrs. Dichloromethane was chosen for this procedure for the following reasons: (a) it is highly miscible with bitumen and toluene, and (b) it is not a good solvent for naphthenic acids — practically all of the surfactants would partition into the aqueous phase (as verified by control tests). As such, there would be a complete phase separation of the drained liquid, with the naphthenic acids dissolved in the top aqueous phase, and the hydrocarbon (bitumen + toluene) reporting to the bottom (dichloromethane) portion of the funnel. After 24 hrs of equilibration, the bottom liquid (toluene and bitumen dissolved in dichloromethane) was drained from the separatory funnel and transferred to a rotary evaporator to remove all solvent (dichloromethane and toluene), leaving only bitumen as the residue. (The "rotovap" was set to operate above the boiling point of toluene and was run for 2 hrs.) From the weight of the glass vial which contained the bitumen residue, the amount of bitumen in the drained liquid, m_{bit}, could be determined. Finally, we define the *washing efficiency* as

$$\frac{\text{mass of contaminant removed}}{\text{mass of original contaminant}} \times 100\%$$

where the "contaminant," which should technically be the diluted bitumen, can also be regarded as the bitumen (since the two are at a fixed ratio). Two additional comments should be made on the washing efficiency as defined: (1) It is not an absolute measure and, as such, should only be used for comparative purposes; (2) as the amount of bitumen used to contaminate the sand was 0.80 g (10% of 8.0 g), the washing efficiency is $(m_{\mathrm{bit}}/0.80) \times 100\%$, where m_{bit} is expressed in grams.

Dynamic Light Scattering

In the course of our investigation, we encountered situations where the sizes of swollen micelles needed to be determined (see Results and Discussions). This was done with the dynamic light scattering (DLS) technique, using multiangle goniometer (ALV CGS-3, Langen, Germany) at a scattering angle of 90°. The laser light scattering cell was immersed in toluene at 25ºC. Such experiments were repeated at least three times for each sample.

3. Results and Discussions

Washing Efficiencies and Shear Rate

Recall the two independent variables of the washing experiments (Figure 1) are: the sodium naphthenates concentration (0 – 100 g/L) and the strength of agitation (low or high shear); the dependent variable is of course the washing efficiency. Figure 2 shows the washing efficiency as a function of the surfactant concentration at low shear.

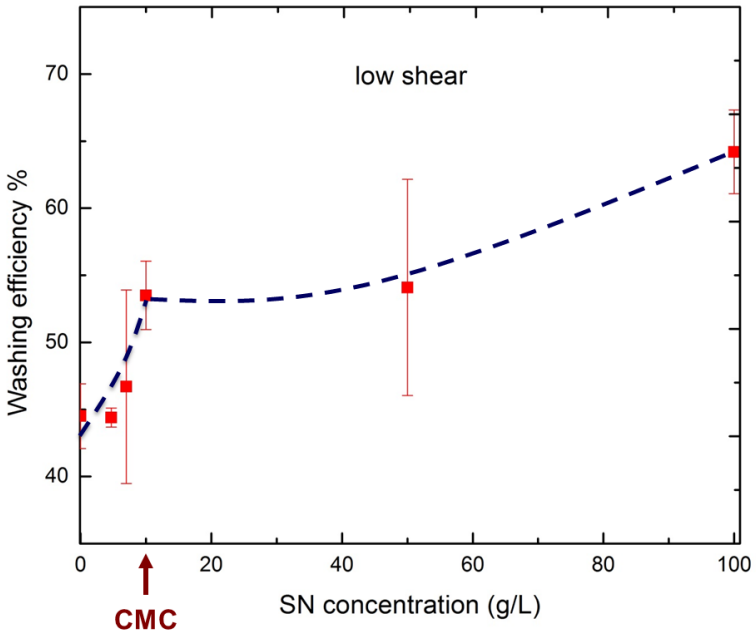

Figure 2. Washing efficiency as a function of sodium naphthenates concentration at low shear rate. The surfactant's critical micelle concentration (CMC) was around 10 g/L. A dashed line is included to show the functional trend; it is not based on any theoretical calculation.

As expected, the washing efficiency increased monotonically with surfactant concentration (i.e. more oil was removed as more surfactants were used). Furthermore, it is noted that the upward trend in Figure 2 is comprised of two distinct regimes, with the transition concentration coinciding roughly with the CMC of the surfactant. This was most likely a consequence of the two mechanisms of emulsification, namely, *dispersion* of the oil below CMC (creating macroemulsions), and *solubilization* above CMC (creating swollen micelles). Next, the same washing experiments were repeated at high shear rate; the results are shown in Figure 3:

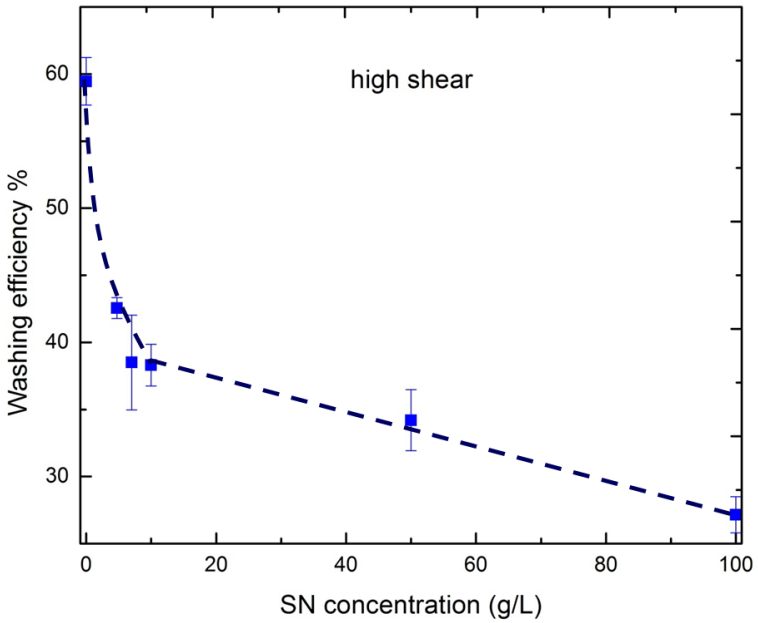

Figure 3. Washing efficiency as a function of surfactant concentration at high shear rate. The dashed line only illustrates the trend and is not a theoretical curve.

Surprisingly, the upward trend in Figure 2, which we were able to rationalize in terms of emulsification mechanisms, is now reversed. The relatively high washing efficiency at zero concentration (i.e. in the absence of surfactants) was perhaps a result of the oil being liberated and dispersed by "brute force." Once surfactants were introduced, however, the data shows a precipitous drop in washing efficiency. The addition of surfactants, which was meant to further facilitate the remediation process, proved to be counter-productive. To investigate this anomaly, we chose to focus on a simpler situation, namely,

interaction between the oil phase and the aqueous phase without the involvement of sand particles.

Appearance of a Third Phase

We mixed 100 g of the oil phase (10 wt% diluted bitumen) with 100 g of the aqueous phase (sodium naphthenates solution at an intermediate concentration of 50 g/L) at the two shear rates described in the Experimental section. The intention of this exercise was to find out whether the oil would emulsify into the aqueous phase, or vice versa. What was observed instead was an unexpected phenomenon shown in Figure 4.

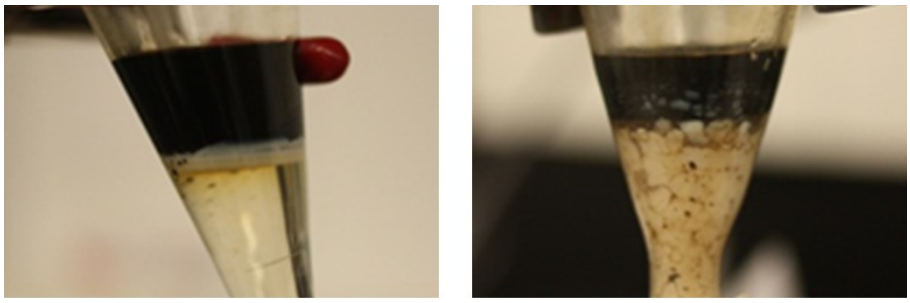

Figure 4. Results of mixing equals amounts of the oil phase (10 wt% diluted bitumen) and the aqueous phase (SN solution at 50 g/L) under (a) low shear, and (b) high shear. Note that the white liquid in (b) was actually quite homogeneous; what appears as "lumps" was due to streaks of black oil that were stuck to the inner wall of the vial.

At low shear, a layer of milk-like liquid was formed at the top of the aqueous phase (Fig. 4a). Like milk, this white liquid was completely miscible with water, but could not mix with the hydrocarbon. By contrast, with vigorous agitation, the

milk-like substance was seen to occupy the entire aqueous domain with a rather opaque white colour (Fig. 4b). Another important observation was as follows: even when quiescent, the "milky layer" in Figure 4a would spontaneously extend downward, on a time scale of ~10 hrs, while maintaining more or less the same opacity (i.e. it did not seem to dilute as its volume expanded). The growth of this milky layer could be greatly accelerated with mechanical shear, leading eventually to a final state that was similar to what is shown in Figure 4b (which was formed in minutes).

From the above observations, a number of deductions can be made. First, the milk-like substance had to be a water-continuous dispersion of liquid droplets or solid particles; let us suppose for now that they were liquid drops (to be justified later). We further deduce that:

1. The droplets were of order 1 μm or larger, which resulted in the emulsion's opacity.
2. The dispersed liquid must be transparent to visible light, hence the white colour of the emulsion. This eliminates the possibility of the droplets being diluted bitumen, which was a very dark liquid.
3. Based on the emulsion's position in Figure 4a, the dispersed liquid must have a density that was intermediate between the densities of diluted bitumen and water.
4. The dispersed liquid was not miscible with either diluted bitumen or water.

Immiscibility with oil and water implied that the dispersed substance existed as a *third phase*. Clearly, this third phase could only be made up of diluted bitumen, water, and/or surfactants. If this material were truly a liquid, there could only be one possibility: it was a bicontinuous (BC) mixture of diluted bitumen and water, facilitated by a significant amount of surfactants which served to lower the oil-water interfacial tension and allow "random mingling" of the two inherently immiscible liquids. When the random mingling is on colloidal length scales, there can be enough entropic contribution for the mixture to become a true (i.e. thermodynamically stable) third phase that is distinct from — and immiscible with — oil and water; this is known as a bicontinuous microemulsion or "BC μE" [8, 18]. In our case, the diluted bitumen content in the BC μE must be quite low, as the third phase was essentially transparent (see Point 2 above). Another important point regarding the BC μE: if it were indeed a thermodynamic state, it should appear spontaneously under conditions which favour its formation (i.e. when the system is in the appropriate region of the phase diagram); as discussed above, this was indeed observed (recall the spontaneous growth of the milky liquid on time scale of ~10 hrs). Creation of the third phase could also be seen in "real time" when the experiment was conducted on shorter length scales.

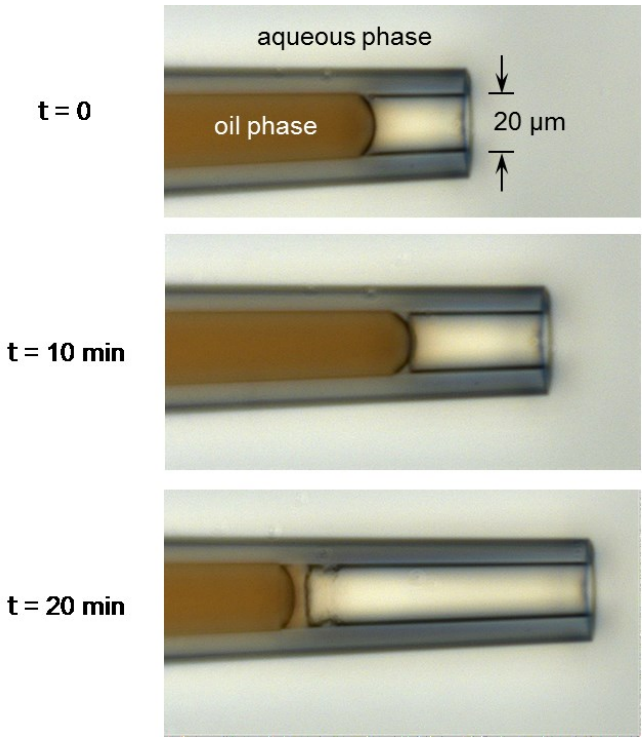

Figure 5. A micropipette filled with diluted bitumen was immersed in an aqueous solution of sodium naphthenates. After several minutes, a third liquid, which was immiscible with oil and water, appeared spontaneously at the oil-water interface.

Figure 5 shows a 20-µm glass pipette that was filled with the oil phase (10 wt% diluted bitumen), then immersed into an aqueous solution of sodium naphthenates (at 50 g/L). As seen, a third phase, which was immiscible with both oil and water, was formed spontaneously at the oil water interface after several minutes. This third phase had a slightly yellowish colour — strong evidence that it was a mix of diluted bitumen and water. Note also that the third phase conformed itself to the shape of the pipette inner wall and the leading edge of the oil, suggesting that it was fundamentally a liquid material (as opposed to rigid substances such as precipitated solid or liquid crystal). Finally, the third phase in Figure 5 was

invisible under cross-polarized light, which indicated that it was an isotropic liquid. All these characteristics were clear evidence that the third phase was a bicontinuous microemulsion.

Effect of the Third Phase on Washing Performance

Unlike the deductions made thus far, the following arguments are more speculative. Our first conjecture is that hydrodynamic shear can function as a *catalyst* which accelerates the formation of BC μE. Though ultimately driven by thermodynamics, the formation of BC μE can be very slow under quiescent conditions. However, mechanical agitation can greatly shorten the time for the system to reach its new equilibrium state (cf. the case from Figure 4a to Figure 4b).

We now turn to washing performance. To begin, it is noted that the BC μE is a highly surfactant-rich structure. Its formation consumes a large amount of surfactants, thus preventing sodium naphthenates from functioning as a remediation agent. At low shear rate (Figure 2), formation of the BC μE was sufficiently slow that most of the surfactants were still available to emulsify the contaminant by either dispersion below the CMC, or solubilization above the CMC. (Here, "slow" implies the time scale of BC μE formation was much longer than that of the washing process.) By contrast, at high shear rate (Figure 3), most of the surfactants were quickly consumed in the creation of the third phase, leaving only few molecules for the emulsification of diluted bitumen. Moreover, an emulsion of the third phase (the milky liquid) may likely obstruct drainage of

liberated oil from the porous sand matrix. Such a scenario is consistent with the downward trend seen in Figure 3.

Disappearance of the Third Phase

In the above discussion, the last conjecture was that dispersed droplets of BC μE (indeed, droplets of any liquid) would create additional resistance to the flow of the suspension. Such a notion is well established in colloid science: the overall rheology of an emulsion depends on factors such as the volume fraction of the dispersed phase, its drop size distribution, the viscosities of the two liquids (here, water and BC μE), their interfacial tension, etc [19]. This suggests a logical next step in our investigation: isolate the milk-like emulsion and examine its various properties — beginning with microscope images of the BC μE droplets and micromechanical tests on the individual drops (such techniques have been developed by our group for other emulsion systems [20, 21]). Unfortunately, all such efforts were futile as the milky emulsion, when isolated from the environment in which it was formed, would "disintegrate" and turn into an aqueous phase. Taking as an example the emulsion in Figure 4b (the milky bottom portion): when kept in the container with the diluted bitumen, it could remain stable for weeks and possibly much longer. However, when the emulsion was drained from the bottom of the vial, the milk-like dispersion turned into a slightly yellow but transparent liquid in 1–2 days. This yellowish liquid was clearly aqueous in nature, as it was miscible with water but not with a hydrocarbon such as toluene. Once again, we found the characteristic time of

such a phenomenon to be much shorter on the micron scale: If observed under an optical microscope (provided the sample was retrieved and viewed quickly), droplets of the third phase, which ranged from microns to tens of microns in size, disappeared within seconds. We believe the disappearance of the third phase can be explained by examining the relative ratios of the oil, water and surfactant components. Initially, the amounts of oil and water in the system were equal, and together they accounted for the majority of the ternary system. However, by removing the diluted bitumen, the oil fraction in the new system (which is now the milky emulsion) had suddenly dropped to almost zero. This caused a major shift of the system in phase space, as shown through a hypothetical ternary phase diagram in Figure 6 below.

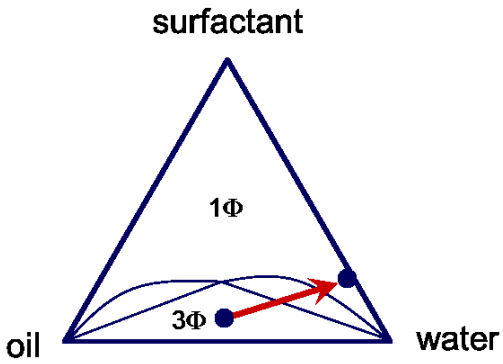

Figure 6. A hypothetical (but typical) ternary phase diagram of a surfactant-oil-water system. By removing the diluted bitumen (the oil), the system undergoes a major shift in phase space as shown — moving from a 3-phase (3Φ) region to a single-phase (1Φ) region of swollen micelles in water.

Figure 6 depicts a typical ternary phase diagram of a surfactant-oil-water system, with the boundary lines separating domains of one-, two-, and three-phase

systems [22]. The arrow in the figure represents the system going from a 3-phase region (the so-called Winsor III system, in which oil, water, and a microemulsion coexist) to a single-phase region (micelles or swollen micelles suspended in water). If this explanation were true, the disappearance of the BC μE droplets would be a result of the surfactants abandoning the bicontinuous structure and existing instead as either monomers or micelles in water. The oil (diluted bitumen) that was originally a part of the bicontinuous structure must now be solubilized by the micelles, thus giving the new aqueous liquid its yellowish colour. As the micelle sizes are on the colloidal scale, the solution appeared transparent to visible light.

We expect an aqueous solution of "disintegrated BC μE" to have the following characteristics: (a) it consists of swollen micelles solubilizing the diluted bitumen, and (b) it is saturated with surfactant monomers in solution *and* at the air-water interface. To check these, we measured the surface tension (using the Wilhelmy plate) and micelle size (using DLS) of the following two aqueous solutions:

- As a control test, we prepared a sodium naphthenates solution at 50 g/L (well above the CMC level of 10 g/L). The surface tension of this solution was 30.8 mN/m, and the micelle size was 3.1 ± 0.3 nm (i.e. the size of an "unswollen" micelle).
- The second aqueous solution was a "disintegrated BC μE" from the bottom portion Figure 4b (see text above the figure for its composition).

The surface tension of this aqueous solution was again 30.8 mN/m, and the micelle sizes ranged from 3.6 to 48.2 nm.

With the micelle sizes in the second solution all larger than that of an unswollen micelle, and given the equality of the surface tensions, we are confident that the disappearance of the BC μE was due to the phase change as depicted in Figure 6.

4. Conclusions

Due to its very favourable interfacial properties (the ability to lower interfacial tension and create hydrophilic surfaces), naphthenic acids was proposed as a surfactant for cleaning oil-contaminated sand grains. However, when evaluated by actual washing experiments, the surfactant proved inadequate as a remediation agent. Specifically, with the inadvertent creation of a bicontinuous "third phase," addition of surfactants to the washing process proved counter-productive at shear rates that are representative of an actual commercial operation (Figure 3). On a broader picture, the ability to lower oil-water interfacial tensions has often been a primary criterion for a surfactant to be effective in soil remediation or chemical enhanced oil recovery; achievement of "ultralow" interfacial tensions and creation of microemulsions have been considered positive traits. This particular case study may offer a cautionary note to such a philosophy.

5. References

[1] Woynillowicz D, Severson-Baker C, Raynolds M. Oil sands fever: The environmental implications of Canada's oil sands rush. The Pembina Institute 2005.

[2] Grant J, Dyer S, Woynillowicz D. Fact or fiction: Oil sands reclamation. The Pembina Institute 2008.

[3] Wu J, Dabros T. Process for solvent extraction of bitumen from oil sand. Energy & Fuels 2012;26(2):1002-8.

[4] Hsieh CR, Clifford RK. Solvent extraction process for recovering bitumen from tar sand. US Patent 1987.

[5] Ang CC, Abdul AS. Aqueous surfactant washing of residual oil contamination from sandy soil. Ground Water Monitoring & Remediation 1991;11(2):121-7.

[6] Mulligan CN, Yong RN, Gibbs BF. Surfactant-enhanced remediation of contaminated soil: A review. Engineering Geology 2001;60(1-4):371-80.

[7] Sheng JJ. Modern chemical enhanced oil recovery theory and practice. New York: Elsevier; 2011.

[8] Sjöblom J, Lindberg R, Friberg SE. Microemulsions - phase equilibria characterization, structures, applications and chemical reactions. Advances in Colloid and Interface Science 1996;65:125-287.

[9] Deshpande S, Shiau BJ, Wade D, Sabatini DA, Harwell JH. Surfactant selection for enhancing ex situ soil washing. Water Research 1999;33(2):351-60.

[10] Abdul AS, Gibson TL, Rai DN. Selection of surfactants for the removal of petroleum products from shallow sandy aquifers. Ground Water 1990;28(6):920-6.

[11] Afshar S, Mirmontazeri L, Yeung A. Potential use of naphthenic acids in soil remediation: Examination of pore-scale interfacial properties. Fuel 2014;116:395-8.

[12] Horvath-Szabo G, Masliyah JH, Czarnecki J. Phase behavior of sodium naphthenates, toluene, and water. Journal of Colloid and Interface Science 2001;242(1):247-54.

[13] Cyr TD, Strausz OP. The structures of tricyclic terpenoid carboxylic acids and their parent alkanes in the alberta oil sands. Journal of the Chemical Society, Chemical Communications 1983;(18):1028-30.

[14] Cyr TD, Strausz OP. Bound carboxylic acids in the Alberta oil sands. Organic Geochemistry 1984;7(2):127-40.

[15] Yang X, Czarnecki J. Tracing sodium naphthenate in asphaltenes precipitated from Athabasca bitumen. Energy & Fuels 2005;19(6):2455-9.

[16] Jin Y, Liu W, Liu Q, Yeung A. Aggregation of silica particles in non-aqueous media. Fuel 2011;90(8):2592-7.

[17] Liu W, Jin Y, Tan X, Yeung A. Altering the wettability of bitumen-treated glass surfaces with ionic surfactants. Fuel 2011;90(9):2858-62.

[18] De Gennes PG, Taupin C. Microemulsions and the flexibility of oil/water interfaces. The Journal of Physical Chemistry 1982;86(13):2294-304.

[19] Tadros TF. Fundamental principles of emulsion rheology and their applications. Colloids and Surfaces A: Physicochemical and Engineering Aspects 1994;9139-55.

[20] Yeung A, Dabros T, Masliyah J, Czarnecki J. Micropipette: A new technique in emulsion research. Colloids and Surfaces A: Physicochemical and Engineering Aspects 2000;174(1-2):169-81.

[21] Moran K, Yeung A, Masliyah J. Measuring interfacial tensions of micrometer-sized droplets: A novel micromechanical technique. Langmuir 1999;15(24):8497-504.

[22] Taupin C, Dvolaitzky M, Ober R. Structure of microemulsions: Role of the interfacial flexibility. Il Nuovo Cimento D 1984;3(1):62-74.